CrossMark

REVIEW

Particle/cell separation on microfluidic platforms based on centrifugation effect: a review

Wisam Al-Faqheri[1] · Tzer Hwai Gilbert Thio[2] · Mohammad Ameen Qasaimeh[3] · Andreas Dietzel[4] · Marc Madou[5] · Ala'aldeen Al-Halhouli[1]

Abstract Particle/cell separation in heterogeneous mixtures including biological samples is a standard sample preparation step for various biomedical assays. A wide range of microfluidic-based methods have been proposed for particle/cell sorting and isolation. Two promising microfluidic platforms for this task are microfluidic chips and centrifugal microfluidic disks. In this review, we focus on particle/cell isolation methods that are based on liquid centrifugation phenomena. Under this category, we reviewed particle/cell sorting methods which have been performed on centrifugal microfluidic platforms, and inertial microfluidic platforms that contain spiral channels and multi-orifice channels. All of these platforms implement a form of centrifuge-based particle/cell separation: either physical platform centrifugation in the case of centrifugal microfluidic platforms or liquid centrifugation due to Dean drag force in the case of inertial microfluidics. Centrifugal microfluidic platforms are suitable for cases where the preparation step of a raw sample is required to be integrated on the same platform. However, the limited available space on the platform is the main disadvantage, especially when high sample volume is required. On the other hand, inertial microfluidics (spiral and multi-orifice) showed various advantages such as simple design and fabrication, the ability to process large sample volume, high throughput, high recovery rate, and the ability for multiplexing for improved performance. However, the utilization of syringe pump can reduce the portability options of the platform. In conclusion, the requirement of each application should be carefully considered prior to platform selection.

Keywords Microfluidic platforms · Cells separation · Particle separation · Lab-on-a-chip · Lab-on-a-disk · Centrifugal effect

1 Introduction

Particle and cell isolation and analysis have drawn more and more interest due to its perceived importance in many different fields and applications (Sajeesh and Sen 2014). In biomedical and biological research, the ability to isolate specific particles and cells from a heterogeneous background is considered a key tool for the study of individual cells or particles. This technology has resulted in great discoveries in cell biology and could be utilized to precisely predict a patient's health status (Tomlinson et al. 2013; Sajeesh and Sen 2014). A case in point is the development of methods to isolate circulating tumor cells (CTCs). CTCs are rare cells that originate from primary cancer tumors and travel through the blood to other sites. This is how cancer spreads to secondary sites and organs in the body. CTCs were first observed in 1869 by Ashworth (1869) and have become a topic of keen interest again in the mid 1990's. The isolation of CTCs can be called "liquid biopsy" as it

✉ Ala'aldeen Al-Halhouli
alaaldeen.alhalhouli@gju.edu.jo

1 NanoLab, School of Applied Technical Sciences, German Jordanian University, Amman, Jordan

2 Faculty of Engineering and Quantity Surveying, INTI International University, 71800 Nilai, Negeri Sembilan, Malaysia

3 Division of Engineering, New York University Abu Dhabi, Abu Dhabi, United Arab Emirates

4 Institut fur Mikrotechnik, Technische Universität Braunschweig, Braunschweig, Germany

5 Department of Biomedical Engineering, University of California Irvine, Irvine, CA, USA

reflects important and early information about tumor status and progress. Other than in the field of cell biology, the use of particle/cell separation has been applied to other applications including the separation of magnetic particles from a background mixture (Kirby et al. 2012), separation and observation of bacteria from host blood cells (Hou et al. 2015), malaria enrichment (Warkiani et al. 2015b), and separation of DNA (Zhao et al. 2015).

The demand for compact, inexpensive, disposable, and high throughput devices that can be implemented for particle/cell separation has led many researchers to consider the various advantages of microfluidic platforms (Burger et al. 2012a). The ability of microfluidic platforms to manipulate small amounts of fluid (on the scale of microliters and below) in micromachined channels has significantly decreased the required volumes of samples and reagents. Although microfluidic devices do feature many advantages, a challenge comes about when large sample volumes must be processed (few milliliters) to increase the chance of isolating rare cells such as CTCs (Amasia and Madou 2010). Furthermore, in most cases some type of enrichment/concentration step is often required.

Various microfluidic methods and procedures have been developed for the isolation of targeted particles and/or cells based on their unique characteristics such as geometry, physical, chemical, or genetic properties. The proposed microfluidic platforms fall under one of two categories according to the operation mechanism: stationary microfluidics, also known as lab-on-chip (LOC) or centrifugal microfluidics, more commonly known as lab-on-disk (LOD). Under the LOD category, different passive and active methods were proposed for particle/cell sorting and isolation. On the other hand, LOC methods mainly rely on the inertial effect for particle/cell manipulation. These methods have the advantages of high throughput, simple design, easy operation, and passive activation without the need for external force for particle/cell manipulation. The different isolation methods are usually evaluated by criteria such as purity, recovery rate, and viability (Tomlinson et al. 2013). Purity represents the degree of contamination of the recovered targeted cells with unwanted background cells/particles. Recovery rate reflects the ratio of number of recovered targeted cells to the number of cells in the original sample, and viability is the number of recovered live and heathy cells, which is very important for subsequent cell analysis stages. Therefore, ideal cell isolation methods should have short processing time, with high recovery and purity rates that result in viable cells.

Many recent detailed reviews are available that highlight available methods for particle/cell isolation with different types of microfluidic platforms (Warkiani et al. 2015c; Hyun and Jung 2014; Tomlinson et al. 2013; Burger et al. 2012a; Sajeesh and Sen 2014). However, this review is focused only on particle/cell isolation methods that are based on centrifugation approaches. Centrifugation approaches presented include methods that utilize the physical centrifugation process on microfluidic platforms, and the approaches that utilize liquid centrifugation effects due to Dean effect for cell/particle separation. The platforms reviewed include the microfluidic CD, and platforms with spiral microfluidics and multi-orifice microfluidics. For a clear view of the categories, please refer to Fig. 1.

2 Centrifugal-base microfluidics for particle/cell isolation

The first step in almost any particle/cell-based research is the isolation and purification of the particles/cells from raw samples such as whole blood or serum. This first step is an important one that needs to produce results in high purity, high recovery rates, and high viability numbers (please refer to the definitions of these three terms in Sect. 1). Various techniques have been implemented to perform particle/cell isolation and purification on microfluidic platforms. In this review, these methods and techniques will be presented and the advantages and disadvantages of each method will be highlighted. According to an extensive review for currently available isolation methods, both centrifugal microfluidic platforms and inertial microfluidic platforms have implemented some form of liquid centrifugation/spinning phenomenon to separate particles/cells from heterogeneous backgrounds. For the centrifugal microfluidic platform, the whole platform is spun with computer-controlled motors to perform different separation methods. On the other hand, inertial microfluidic platforms utilize special structure of microchannel such as curved channels or channels with sudden expansion–contraction arrays to generate secondary centrifugation flow to separate particles/cells based on their physical properties.

The next section of this paper is divided into two main sections: centrifugal microfluidic platforms and inertial microfluidic platforms (see Fig. 1). In the first section, the separation methods are classified into passive methods (separation without the need for an additional external force) and active methods (separation using an external force). In the following section, i.e., inertial microfluidics methods, the methods are all passive, and the classification is based only on channel structure. The methods rely on either spiral or multi-orifice channels to execute particles/cells separation.

2.1 Centrifugal microfluidic platforms

Centrifugal microfluidic platforms are circular-shaped platforms containing a network of microchannels and
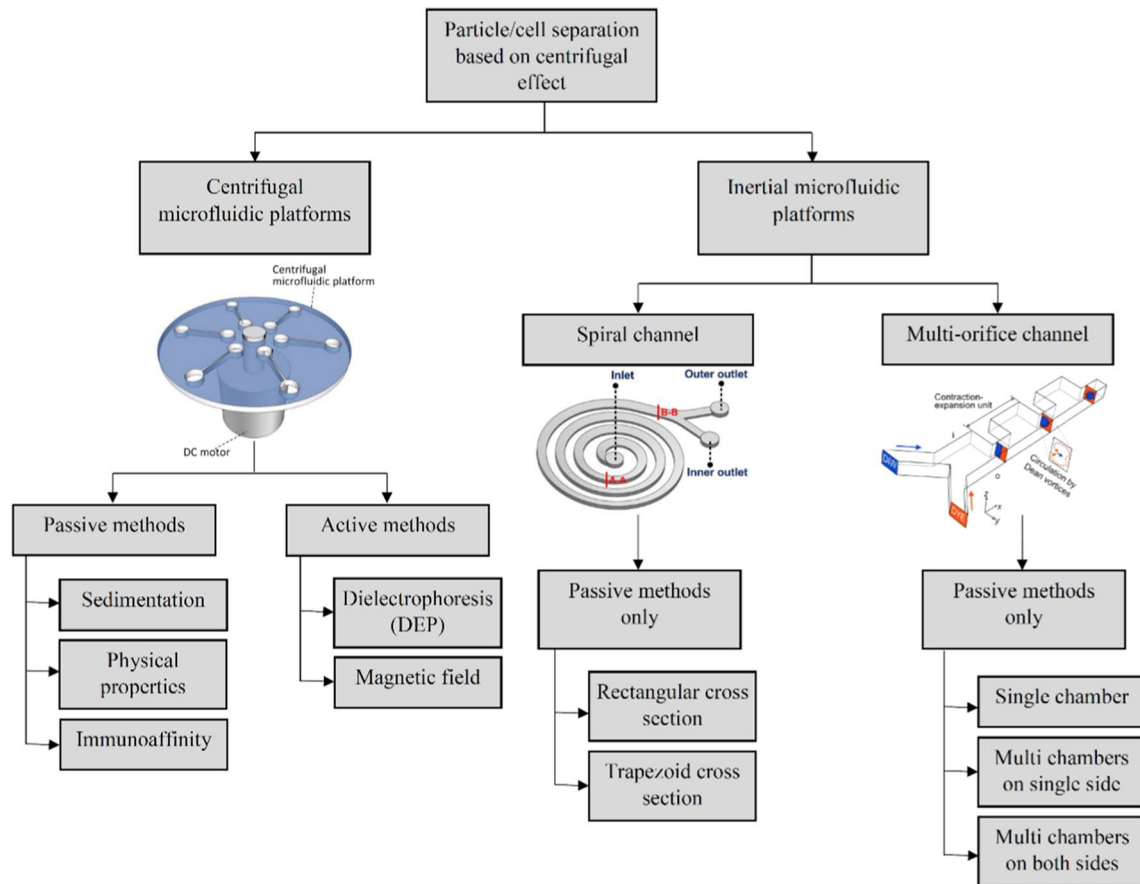
Fig. 1 Cell separation methods on microfluidic platform based on centrifugation effect. Spiral figure is adopted from Warkiani et al. (2015a) under a Creative Commons Attribution 4.0 International License, and multi-orifice figure is adopted from Lee et al. (2009a) with permission from AIP Publishing LLC

Fig. 2 Centrifugal microfluidic platform preloaded with a volume of liquid in a straight microfluidic channel. The figure highlights the main forces acting on the loaded liquid, i.e., centrifugal force (pushing liquid toward the outer edge of the platform), capillary force (acting against liquid flow), Coriolis force (perpendicular to the liquid flow and opposite to rotation direction), and Euler force (perpendicular to the CD rotation direction)

$$\Delta r = r_2 - r_1$$
$$\bar{r} = (r_1 + r_2)/2$$
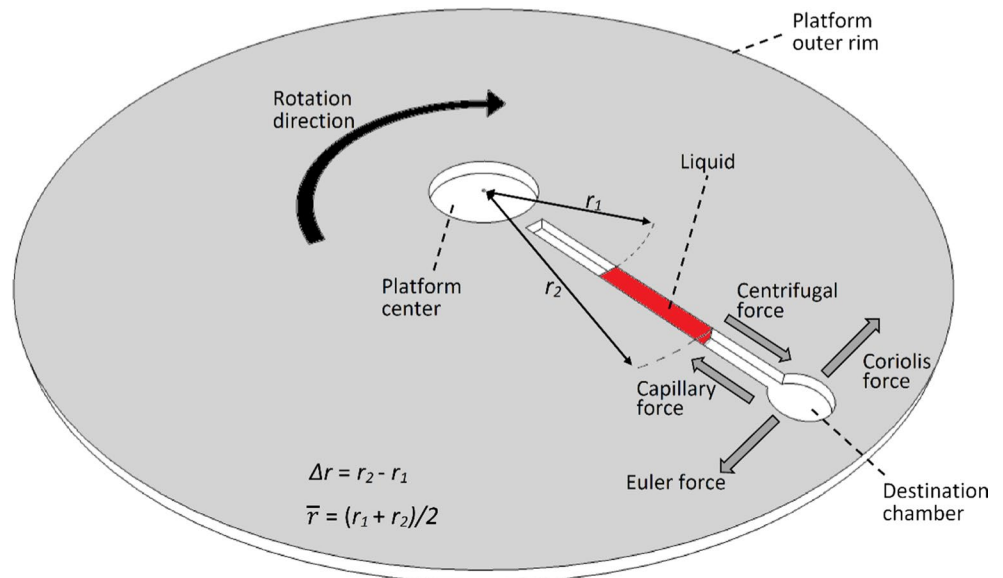
chambers. Figure 2 shows a simple design of the platform with a single straight microchannel leading away from the center of the platform toward a chamber. As the platform resembles a compact disk (CD), it is commonly referred to as the centrifugal microfluidic CD.

The main fluidic propulsion force on the CD is the centrifugal force resulting from the spinning of the CD (Madou et al. 2006; Burger et al. 2012a; Strohmeier et al. 2015a; Smith et al. 2016; Tang et al. 2016). As the CD is spun, the centrifugal force applies outward pressure on fluids in the CD and propels fluids toward the CD edge. The centrifugal force per unit volume and the resulting pressure can be determined as follows (Madou et al. 2006; Ducrée et al. 2007):

$$F_{\text{cen}} = \rho \omega^2 \bar{r} \tag{1}$$

$$P_{\text{cen}} = \rho \omega^2 \Delta r \bar{r} \tag{2}$$

where ρ is the density of preloaded fluid, ω is the CD spinning speed in radians per second (rad/s), Δr is the difference between the top and bottom levels of a volume of fluid relative to the CD center, and $\bar{r}$ is the average distance of the column of fluid from the CD center.

Under the centrifugal pressure, the average velocity of fluid on the CD can be determined as follows (Smith et al. 2016):

$$U = \frac{D_{\text{h}}^2 P_{\text{cen}}}{32 \mu L} \tag{3}$$

where D_{h} is the hydraulic diameter of the channel or chamber the fluid is flowing in, μ is the viscosity of the fluid, and L is the length of the column of fluid on the disk.

To prevent all fluids from running toward the CD edge without any order or sequence, specially designed passive valves are placed along channel paths (Thio et al. 2013). On hydrophilic CDs, the most commonly employed passive valve is the capillary valve. A capillary valve is characterized by any sudden opening along the microchannel, such as the microchannel opening to a chamber shown in Fig. 2. As fluid flows under the effect of centrifugal force toward the boundary of a capillary valve, the capillary force applies opposing pressure on the fluid. This capillary pressure can be determined with the following mathematical expression (Thio et al. 2013):

$$P_{\text{cap}} = \frac{4 \cos \theta_{\text{c}} \gamma_{\text{la}}}{D_{\text{h}}} \tag{4}$$

where θ_{c} is the fluid to surface contact angle and γ_{la} is the fluid–air surface energy.

When centrifugal and capillary pressures are at equilibrium, fluid is stopped at the boundary of the microchannel and valve. For any fluid to flow past any capillary valve, the centrifugal pressure, P_{cen} must overcome the capillary pressure, P_{cap}. Most parameters that affect P_{cen} and P_{cap} are constants based on valve location on the CD, and also on fluid and CD material properties. The only parameter that can be freely adjusted to disrupt the equilibrium between P_{cen} and P_{cap} is the CD spinning speed. To design a network of microchannels and valves that allow for a series of fluid movement on the CD, the minimum CD spinning speed where the centrifugal pressure exceeds the capillary pressure for each valve needs to be determined. This CD spinning speed is commonly referred to as the burst frequency and is usually presented in revolutions per minute (rpm) as follows (Thio et al. 2013):

$$\text{rpm} = \sqrt{\frac{P_{\text{cap}}}{\rho \Delta r \bar{r}}} \left(\frac{30}{\pi} \right) \tag{5}$$

On the CD, apart from the centrifugal force, there is also the Coriolis, the Euler, and a secondary centrifugal forces acting on fluids in the platform. The Coriolis force is perpendicular to the velocity of the moving fluid and is frequently used for switching the lateral flow direction on the CD, and also for density-based particle separation and sorting (Burger and Ducrée 2012; Kim et al. 2008; Brenner et al. 2005). The Coriolis force per unit volume can be determined as follows (Ducrée et al. 2007):

$$F_{\text{corr}} = 2 \rho \omega U \tag{6}$$

The direction of the Euler force is opposite of the CD spinning acceleration and perpendicular to the centrifugal force and can be used to create lateral motion of fluid during disk acceleration for mixing applications (Smith et al. 2016). The Euler force per unit volume can be determined as follows (Ducrée et al. 2007):

$$F_{\text{eur}} = \rho \bar{r} \frac{d\omega}{dt} \tag{7}$$

The secondary centrifugal force is only present in curved microchannels and supplements the main centrifugal force. This secondary force can be used for particle separation and can be determined as follows (Zhang et al. 2008):

$$F_{\text{sec}} = \rho u^2 / R \tag{8}$$

where u is the velocity of the fluid flow in the channel and R is the radius of the curvature of the curved channel.

Many advantages especially for biological sample handling and cell manipulation were demonstrated on the centrifugal platform (Burger et al. 2012a). Three of these advantages that apply to cell manipulation are listed here:

1. Simple implementation of sedimentation for sample separation and cell enrichment (concentration) by utilizing the centrifugation process (Smith et al. 2016).

2. Centrifugation pumping is highly independent of sample properties such as viscosity, electrical conductivity, and pH, which is ideal for handling biological samples such as blood (Madou et al. 2006; Warkiani et al. 2015c).

3. Clear separation between the microfluidic networks and the pumping/detection components prevents sample contamination and improves the disposability of the platform (Burger et al. 2012a; Warkiani et al. 2015c).

In the following two sections, the main passive and active methods for particle/cell separation on the centrifugal microfluidic platforms are discussed. The main proposed methods are summarized in Table 1 with their utilized methods, processed samples, and reported results.

2.1.1 Passive particle and cell separation methods

Many passive techniques to perform particle/cell isolation on the centrifugal microfluidic platform have been reported. In several of these reports, centrifugal microfluidic platforms were proposed as an alternative to conventional benchtop centrifugation devices to separate blood components (Riegger et al. 2007; Steigert et al. 2006, 2007; Haeberle et al. 2006; Lee et al. 2011a; Zhang et al. 2008; Kim et al. 2013; Kinahan et al. 2014b; Park et al. 2014; Amasia and Madou 2010). The various techniques can be categorized into three types (1) sedimentation- or density-based blood fractionation (Park et al. 2008, 2014; Kinahan et al. 2014a, b; Nwankire et al. 2015b; Burger et al. 2012a; Haeberle et al. 2006; Li et al. 2010; Kim et al. 2013; Steigert et al. 2007; Strohmeier et al. 2015b), (2) cells/particles separation based on physical properties, and (3) separation based on immunoaffinity processes.

2.1.1.1 Density-based blood fractionation (sedimentation)

The importance of blood as the biological sample for most diagnostic assays, and the need for portable devices with high throughput to handle blood samples is the main driver behind the high number of research articles in this area. In particular, one of the most investigated blood separation methods on centrifugal microfluidic platforms is the isolation of the plasma portion from the rest of the blood cells portion (Strohmeier et al. 2015b). According to Strohmeier et al. (2015b), the plasma separation process can be divided into two main steps: (1) cell sedimentation by centrifugation and (2) plasma extraction from the layer-separated sample. The plasma separation step is usually performed in a sedimentation chamber or in another microstructure that is positioned radially on the centrifugal microfluidic platform (Park et al. 2008, 2014; Kinahan et al. 2014a; Nwankire et al. 2015b; Burger et al. 2012a; Haeberle et al. 2006; Li et al.

2010). This configuration of the sedimentation chamber forces the higher density portion of the blood (blood cells) to settle at the bottom of the chamber during centrifugation. The lighter portion of the blood (plasma) stays at the top of the blood cells layer. Kim et al. (2013) and Kinahan et al. (2014b) investigated the effect of the sedimentation chamber geometry on the purity, and the time it takes to perform plasma separation (see Fig. 3). Kim et al. (2013) found that by narrowing the sedimentation channel and enlarging the tilt angle of that channel with respect to the radial direction, the separation process could be sped up to 8 times faster. This can be explained by Boycott's discovery in 1920 when he found that particles sediment faster in tilted chambers due to the larger available surface area for particles to settle on (the side wall and base of the chamber) (Boycott 1920). Another reason the sedimentation process will be faster is due to the shorter distance that the particles/cells need to travel to reach chamber wall compared to the chamber base. This is similar in narrower chambers where the side walls will be closer to each other. Figure 3a–c shows the difference between straight and tilted sedimentation channels. Kinahan et al. (2014b) proposed a curved design of the sedimentation chambers using a logarithmic spiral or mirabilis design (see Fig. 3d–f). The authors claimed that this design can improve the separation process speed by 39% compared to straight sedimentation chambers. This is due to the fact that spiral designs provide not only more surface area for sedimentation (similar to a tilted chamber), and there is also constant centrifugal force applied along the entire channel length compared to varying centrifugal force along tilted chambers.

In separate studies, Li et al. (2010) discussed that after plasma separation is performed using the centrifuge method, blood cells may diffuse into the already separated plasma when the spinning process is stopped (at the end of the centrifuge process). To overcome this problem, the authors proposed out-of-plane microvalves and triangular obstacle structures (TOS). Zhao et al. (2015) proposed a different passive method of using stored pneumatic energy for particles/liquid sedimentation, resuspension, and transport on a centrifugal microfluidic platform. The proposed method is independent of particle size and does not require any external force or special coating of the microfluidic structure. The whole process is purely controlled by the spinning speed of the platform. This method is proposed to improve particle-based assays such as Deoxyribonucleic acid (DNA) extraction and immunoassays.

After the sedimentation process is completed, purified plasma decantation or extraction and subsequent steps are carried out. The extraction step is usually accomplished by utilizing a siphon channel (Steigert et al. 2007; Strohmeier et al. 2015b; Nwankire et al. 2015b), or a straight channel, the latter is controlled by a valve (Park et al. 2008, 2014;

Table 1 Particle/cell separation methods on centrifugal microfluidic platforms

Category	Method	Structure	Sample	Reported results	Remarks
Passive methods	Sedimentation	Straight sedimentation chamber (Amasia and Madou 2010)	Blood (fractionation)	PSV 2 mL, PT 2.5–10 min, SS 3800 rpm, SP 99%	–
		Tilted/spiral sedimentation chamber (Kim et al. 2013; Kinahan et al. 2014b)	Blood (fractionation)	PT 30–180 s, SS 3600 rpm	DGM is used in spiral chambers. Spiral camber improves processing time up to 39% compared to straight tilted chambers
		Curved channel (Zhang et al. 2008; Kuo and Li 2014; Kuo and Chen 2015)	Blood (fractionation)	PSV 0.5–1 µL, PT 1–6 s, SS 1550–1800 rpm, SP 96–99%	Low sample volume, but fast and direct extraction of plasma without the need for siphoning process
	Physical properties	Filter (Lee et al. 2014)	Cells (CTCs)	PSV up to 3 mL, PT 20–30 s, SS 1200–3600 rpm, 61% capture efficiency	30 s is the processing time for cells filtration only. Staining cells can require 1 h
		Serial gaps (Glynn et al. 2015)	Cells (CTCs)	PSV 4 µL, PT 40 min, SS 720 rpm	This method only utilized to distribute different cluster size of cancer cells. Sample was preprocessed to extract other type of cells (white/red blood cells)
		Counterflow centrifugal elutriation (CCE) (Morijiri et al. 2013)	Cells/particles	PSV 5–20 µL, PT 300–720 s, SS 1500–2000 rpm	–
		Zig-Zag channel with u-shaped traps (Kubo et al. 2009; Furutani et al. 2010)	*Escherichia coli*, baker's yeast, Jurkat cell, and NIH3T3 cell	PSV 24 µL, PT 30–40 s, SS 3000–5000 rpm	–
	Immunoaffinity	Centrifugation + density gradient medium (Park et al. 2014)	Cells (CTCs)	PSV 5 mL, PT 78 min, SS ~2300 rpm, Recovery and viability >90%	The proposed setup integrates immunoaffinity and DGM for CTCs capturing and separation
		V-shaped traps (Burger et al. 2011, 2012b)	HeLa, MCF7, RPMI-8226 cells, and beads	PSV 2 µL, PT ~10 min + 90 min incubation time, SS 1200 rpm, BCE = 99%	–
		Micromixer + inertial sorter (Aguirre et al. 2015)	Cells (MCF7)	SS 225 rpm, 97.1% cells/beads binding efficiency, 98% separation efficiency	The proposed platform integrates two unit operations: micromixer (for binding process), and inertial flow (for focusing process)
Active methods	Dielectrophoresis (DEP)	Straight channel + carbon-DEP electrodes (Martinez-Duarte et al. 2010)	Yeast cells	PSV 50 µL, PT 1–16 min, SS 100–175 rpm, flow rate 0.01–0.03 mL/min, filtration efficiency ~100%	Carbon-electrode is integrated on centrifugal platform for improved filtration efficiency
	Magnetic field	Fork-like chamber + integrated magnets (Siegrist et al. 2011; Kirby et al. 2012, 2015)	MCF-7 cancer cells/magnetic particles	PSV 3 µL, PT 10 min, SS 1020 rpm, BCE 90–96%,	–

PSV processed sample volume, *PT* processing time, *SS* spinning speed, *SP* separation purity, *BCE* bead capture efficiency
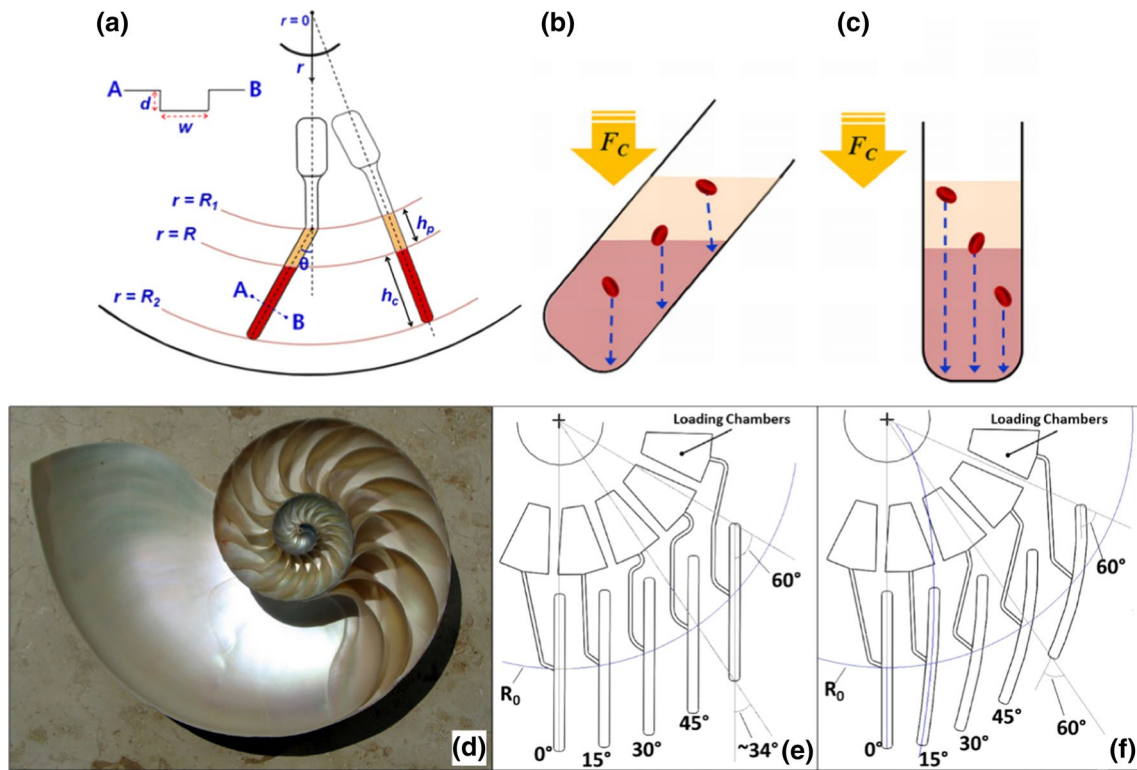
Fig. 3 Isolation of plasma portion from the rest of blood based on centrifugation/sedimentation process; **a–c** effect of tilted sedimentation chamber on plasma separation, **d–f** effect of using a spiral mira-

bilis sedimentation chamber. **a–c** is adopted from Kim et al. (2013) with permission from Elsevier, and **d–f** Is adopted from Kinahan et al. (2014b) with permission from Elsevier

Kinahan et al. 2014a). The intersection of the extraction channel with the sedimentation chamber is positioned slightly above the interface between the layers of plasma and red blood cells (RBC). Compared to a straight channel where an active valve is required, the siphon channel can be passively actuated. When the spinning speed of the platform is decreased, the hydrophilic property of the siphon channel pulls the plasma into the channel and through the crest of the channel. Increasing the spinning speed then push the plasma into the collection chamber.

In different mechanism for plasma/cells separation, Zhang et al. (2008) proposed a simple microfluidic design to separate blood plasma from the other components of the blood. The proposed design consists of a short straight microchannel that leads to a curved microchannel, followed by two collection reservoirs, one for plasma and the other for red blood cells (RBC) reservoir (see Fig. 4). In this system, the blood components will also be under the effect of not just the centrifugal force (f_ω) and the Coriolis force (f_C), but also the secondary centrifugal force (f_R) due to the curvature structure of the microchannel. According to Zhang et al. (2008), the three forces contribute in different degree to the separation process. As blood sample flows through the microfluidic

networks, the blood cells will be forced to flow closer to the outer wall of the microchannel which is nearer to the CD edge, while plasma flows closer to the inner wall of the microchannel which is nearer to the CD center. This is because blood cells have higher density, while plasma has a lower density. At the final Y channel junction, the two parallel flowing layers of blood cells and plasma will flow to separate collection chambers (see Fig. 4). The authors reported a separation efficiency of 90% for blood with 5% hematocrit level, while separation efficiency drops to 65% when whole blood is processed (48% hematocrit). (Kuo and Li 2014; Kuo and Chen 2015) utilized the same basic design and concept by Zhang et al. (2008), but with an extended secondary microfluidic process where the extracted plasma is mixed with specific reagent. Kuo and Li 2014; Kuo and Chen 2015 utilized siphoning and mixing structures to perform prothrombin time (PT) tests. In their follow-up work, the authors implemented a slightly different design with decanting chamber to perform creatinine test. The authors reported high separation efficiency of 96% with a short processing time of 5–6 s, which is dramatically faster when compared to conventional benchtop procedures. Compared to the earlier described sedimentation methods, the curved
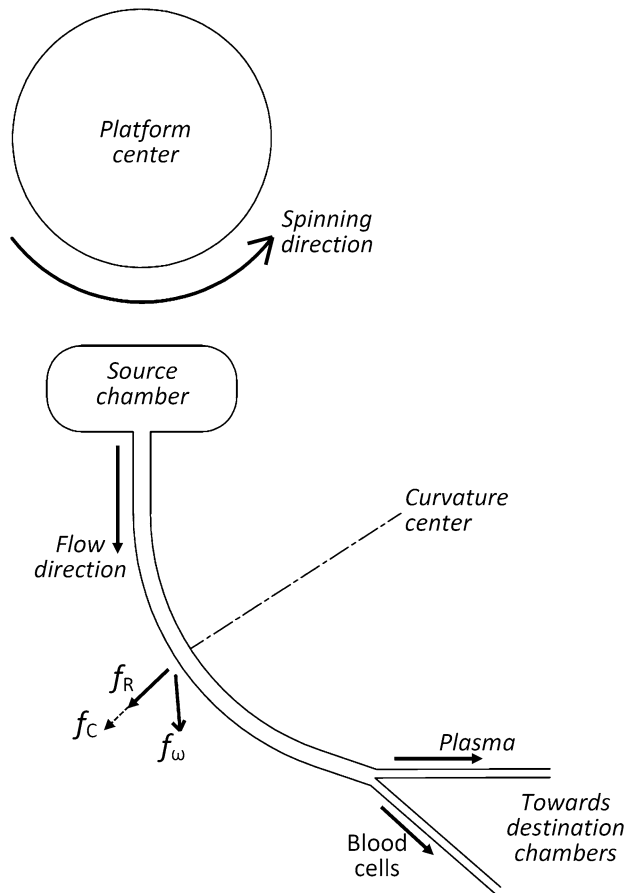
Fig. 4 Blood fractionation using curved channel on centrifugal microfluidic platform is utilized to separate blood plasma from the other components of the blood, f_ω centrifugal force, f_R centrifugal force due to channel curvature, f_C Coriolis force

channel method does not require complex microfluidic design with siphon channels to extract plasma from the layered blood sample.

In a later work by Shamloo et al. (2016), a curved channel with one initial container and three output containers was implemented for cells sorting from blood samples. In their work, a diluted blood sample containing a mixture of RBCs and neutrophils attached to activated magnetic beads is injected into the initial container. As the platform starts spinning, the effects of the centrifugal force, Coriolis force, Euler force, magnetic force and other forces correlated with the curvature structure will transfer the RBCs, bonded neutrophils, and free magnetic beads into different destination containers. The authors reported 100% separation efficiency in an optimum angular velocity of 45 rad/s.

In summary, passive sedimentation of plasma/cells is one of the most important features of the centrifugal microfluidic platforms that allow for full integration of biological

multi-step assays in automated fashion without the need for external interaction such as high trained clinical technician.

2.1.1.2 Cells/particles separation based on physical properties In the previous section, we presented different microfluidic methods for isolating cells in general from blood plasma. Here, we present isolation methods for isolating specific types of cells/particles from a relevant background population. These methods are usually implemented for the enrichment of specific targeted cell type while discarding unwanted cells.

Geometry-based methods for cells and particles isolation on centrifugal microfluidic platforms have been reported in various works. Among the proposed mechanisms are: (1) membrane filter (Lee et al. 2014), (2) filter-like microstructures such as obstacle arrays (Nwankire et al. 2015a) and scale-matched gaps (Glynn et al. 2015), (3) counterflow centrifugal elutriation (CCE) (Morijiri
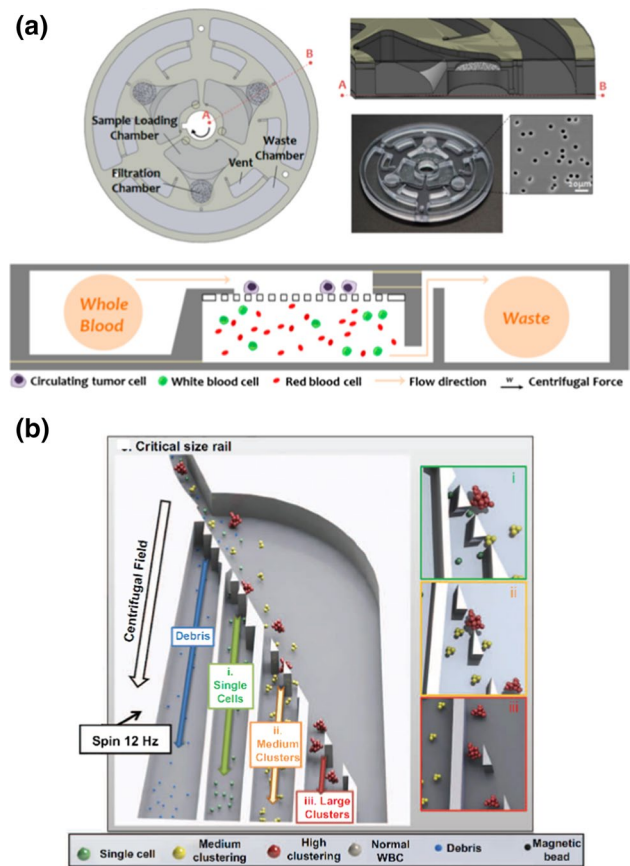

Fig. 5 Particle/cell separation based on its physical properties. **a** Cell separation using membrane filter, microfluidic CD contains three sets, each set with loading chamber, filtration chamber, and waste chamber (Lee et al. 2014). **b** A rail of gaps with increasing opening size is proposed to measure the size distributions of CTCs clusters. **a** is adopted from Lee et al. (2014) with permission from American Chemical Society, **b** Glynn et al. (2015) under a Creative Commons Attribution 4.0 International License

et al. 2013) (4) microchannels with gaps-array (Kubo et al. 2009; Furutani et al. 2010), (5) centrifugal deterministic lateral displacement (c-DLD) (Jiang et al. 2015), density gradient free nanoparticles separation (Arosio et al. 2014), and separation based on density gradient sections (Moen et al. 2016).

Lee et al. (2014) proposed a centrifugal platform for CTCs isolation with three processing sets, where each set contains a sample loading chamber, a filtration chamber, and a waste chamber (Fig. 5a). A commercially available membrane filter with pore size of 8 μm was integrated in the filtration chamber to trap the targeted CTCs. The platform is validated with MCF-7 breast cancer cell line spiked in phosphate-buffered saline (PBS) and blood samples collected from healthy donors. In addition, blood samples from patient with lung and gastric cancers were tested for clinical validation. The process was reported to takes only 20 s to filtrate 3 mL of sample. However, the postprocessing which includes the washing, blocking, incubation, staining, and cell analysis steps takes around 50 min. The authors reported high CTCs capturing efficiency of 84% at relatively low spinning speed of 600 rpm. However, operating the platform at low spinning speed results in a high count of 3092 captured WBC. Meanwhile, at high spinning speed of 3600 rpm, the CTCs capturing efficiency drops to 50% while the WBC count drops significantly to 181 cells. Finally, the authors validated their system experimentally by comparing it with ScreenCell®, the only commercially available microfluidic platform for CTCs isolation. In comparison, the capture efficiencies for the proposed platform and ScreenCell system were 56 and 69%, respectively. The authors believe that the slightly higher efficiency of ScreenCell® system is due to (1) the smaller pore size of the utilized membrane filter of 7.5 μm and (2) the implementation of dilution FC2 buffer which is known to stabilize the cells. This proposed microfluidic platform is the only system which was validated by experimentally and compared to an commercially approved CTCs separation system. Figure 5b presents a novel design proposed by Glynn et al. (2015) to measure the size distributions of CTCs clusters in a blood sample. The authors implemented a rail of gaps with increasing opening size to isolate different clusters based on size variation before sending them to different destination chambers. Morijiri et al. (2013) implemented the counterflow centrifugal elutriation (CCE) method on a centrifugal microfluidic platform for particles sorting based on particle size. The method relies on the balancing of the centrifugal force which pushes particles toward the platform edge, and liquid drag force which pushes particles toward the platform center. As the net force is higher near the chamber inlet and lower near the chamber outlet, bigger particles tend

to flow near the chamber inlet while smaller particle tend to flow toward the chamber outlet. The authors successfully isolated polymer particles of 1, 3, and 5 μm in diameter, and also demonstrated the ability of separate blood cells (erythrocytes and leukocytes) from diluted blood sample. To reach single-cell level analysis on centrifugal platforms, Kubo et al. (2009) proposed a zig-zag-shaped microfluidic channel with U-shaped trapping chambers lined along the sides of the channels. The proposed platform was made of PDMS with a total of 24 microchannels, each with 530 trapping chambers. Various cell types, i.e., *Escherichia coli*, baker's yeast, *Jurkat cell*, and *NIH3T3*, were isolated on the proposed platform at 3000 rpm and 30 s processing time. In a separate study, Jiang et al. (2015) utilized deterministic lateral displacement (DLD) on centrifugal platform for passive particle isolation. On the platform, the authors integrated a square array of cylindrical posts that are in specific tilting angles with respect to the centrifugal force direction. By testing the effect of different tilting angles, the authors found the best scenario when big particles are trapped by arrays with small migration angles while small particles are free to travel following the direction of the centrifugal force. The integration of DLD on the centrifugal platform improves the portability of the developed platform with the elimination of external pumping methods and physical connections. This allows the integration of DLD as a preparation step for cell labeling and/or analysis on the platform. On a nanoparticle level, Arosio et al. (2014) proposed the installation of a simple curved channel with seven collection bins/chambers onto a centrifugal base. The collection bins/chambers are placed in an orientation perpendicular to the centrifugal force direction. As a result, the separation mechanism is based on the balance of the fluid drag force on one side, and the centrifugal and buoyancy forces on the other side. As the analyte with dispersed nanoparticles flow through the separation channel, the centrifugal force will drive big and high density particles to move laterally toward the outer wall of the channel. Smaller and low density particles will experience slower laterally flow speeds and will stay closer to the channel center. Separation of 50, 100, and 200 nanosized particles, at 5000 rpm spinning speed and 5 min processing time, was performed to demonstrate the capability of the proposed system.

In a more recent study, Moen et al. (2016) reproduced the traditional density media and relative centrifugal forces (RCF) procedure for cell separation on the centrifugal microfluidic platform. Moen et al. (2016) proposed a single straight channel that divided into five multiple sections. Each section has a different density media and separated from the neighboring sections by passive capillary valves. This multi-density setup forces different cells

to sediment at different sections based on their respective density. This is due to the different effect of the centrifugal force and liquid drag force on particles of different densities. The authors reported 95.15% recovery rate for leukocytes while excluding 99.8% of red blood cells.

2.1.1.3 Separation based on or for immunoaffinity processes In general, immunoaffinity is defined as the utilization of surfaces or particles that are pre-activated with specific antigens/antibodies which only capture specific targeted cells/proteins. This trapping process facilitates the isolation and sorting of the targeted cells/proteins from heterogeneous background mixtures. In most proposed sorting platforms, immunoaffinity is performed together with other sorting mechanisms such as density gradient medium (DGM) (Park et al. 2014), capture-array (Burger

et al. 2011, 2012b), and waved microchannel for inertial sorting (Aguirre et al. 2015).

Park et al. (2014) from Samsung Biomedical Research Institute developed a fully automated centrifugal microfluidic platform for isolating CTCs from blood samples (see Fig. 6a). The platform designed consists of a blood chamber, a density gradient medium (DGM) chamber, and a collection chamber. Inside the blood chamber, a triangular obstacle structure (TOS) is introduced to prevent blood cells from flowing backward during the plasma evacuation process. The proposed platform has the ability to handle relatively high volume of fresh blood, up to 5 mL, to perform CTCs isolation without any preprocessing or external intervention. The process starts with the introduction of 5 mL of blood sample mixed with 100 µL of 4.5-µm-diameter superparamagnetic
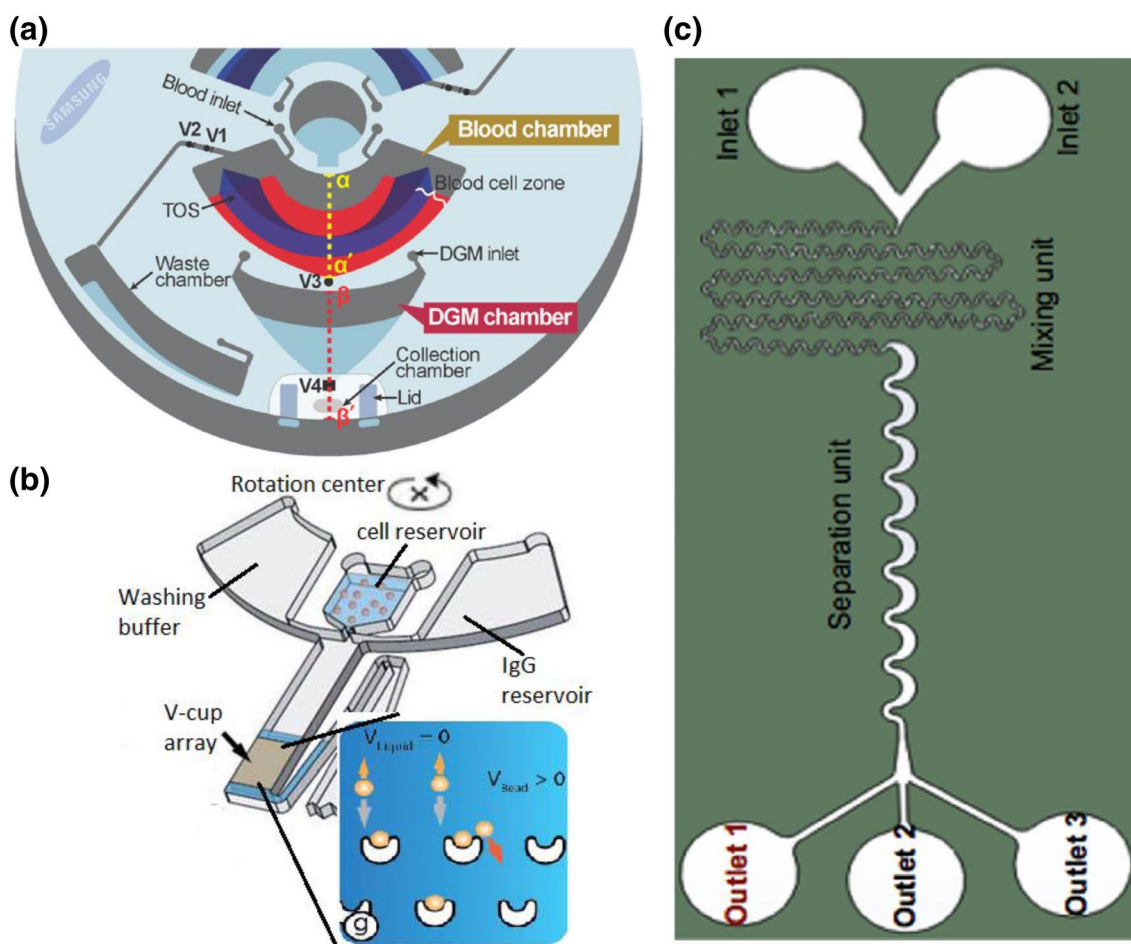

Fig. 6 Immunoaffinity on centrifugal platform for particle/cell separation **a** microfluidic design is proposed for CTCs isolation from blood sample, the design consist of blood chamber, DGM chamber, collection chamber, and waste chamber, **b** microfluidic design with V-shaped traps array is proposed for bead-based assays, the design consist of cell reservoir, washing buffer reservoir, IgG reservoir, V-cup array, and waste chamber, **c** micromixer and inertial sorter are integrated for cancer cells separation based on immunoaffinity. **a** is adopted from Park et al. (2014) with permission from American Chemical Society, **b** is adopted from Burger et al. (2012b) with permission from Royal Society of Chemistry, **c** is adopted from Aguirre et al. (2015) with permission from Springer

activated microbeads used for CTCs trapping. Then, the platform is spun for few minute to separate plasma from the rest of the blood. Plasma is then transferred to the waste chamber, and CTCs is left to bind with the activated microbeads under a simple shaking process. Afterward, the mixture is released to reach the DGM layer where the CTC-bead complex moves down to reach the collection chamber. The authors reported a high recover rate of >95% with >90% cells viability. In separate studies, Burger et al. (2011, 2012b) proposed a centrifugal microfluidic platform for efficient trapping and analysis of particles, which can facilitate bead-based assays (see Fig. 6b). The operation principle of the platform is based on stopped-flow sedimentation, where microparticles are injected into the designated chamber that is filled with stagnant fluid. When the platform is spun, the resultant centrifugal force will force the randomly dispersed particles to flow though the array of V-shaped traps. To demonstrate the ability of the proposed system, the authors performed a single step antibody assay.

A more recent work by Aguirre et al. (2015) reported the integration of two operation units on the centrifugal microfluidic platform. The first unit is a micromixer used to create breast cancer cells and beads complex MCF7-PS. The second unit is an inertial sorter used to isolate cancer-beads complex from the background mixture. The platform design is shown in Fig. 6c. The biological sample of MCF-7 + DMEM culture media, and the anti-Epcam functionalized beads are first injected through inlet 1 and 2. The platform is then spun at an angular velocity of 3.75 Hz to flow the biological sample and microbeads through the micromixer. The proposed micromixer works based on the principle of secondary flow generated by Dean drag force, while cell sorting mechanism is based on lateral migration effect. The authors reported mixing and recovery rate of 97.1 and 98.7%, respectively.

2.1.2 Active particles/cells separation methods

In contrast to passive separation methods which mainly depend on the microfluidic structure and particle physical properties for separation process, active separation methods usually utilize external forces or actuators to facilitate the separation process (Madou et al. 2006; Strohmeier et al. 2015a). In a study by Martinez-Duarte et al. (2010), dielectrophoresis (DEP) was used on the centrifugal microfluidic platform for active filtration and trapping of targeted cells (see Fig. 7a). The authors reported the fabrication and integration of 3D carbon electrodes that resulted in high filtration efficacy with low fabrication cost. The carbon electrodes were supplied with a voltage supply of 200 kHz and 20 V_{pp}. At a sample flow rate of 35 μL/min, the authors successfully separated yeast from

a background mixture of yeast and latex cells with 100% separation efficiency. In separate researches by Kirby et al. (2012, 2015) and Siegrist et al. (2011), magnetic field was imposed on the centrifugal platform for cells manipulation in stopped-flow sedimentation mode. The presented separation methods contain common features such as a source chamber, a focusing channel, and a fork-shaped separation chamber that splits different cell types into different destination sub-chambers (see Fig. 7b). Under the influence of Stokes' drag, centrifugal, and magnetic forces, different cells are guided into the different destination sub-chambers. Using functionalized magnetic beads with anti-EpCAM antibodies, Kirby et al. (2015) reported the isolation of rare MCF7 cancer cells from 3 μL of whole blood at a recovery rate of 90–96%.

2.2 Inertial microfluidics

2.2.1 Spiral microfluidic platforms

Segre (1961) observed that particles with 1-mm diameter are randomly dispersed when flowed through an arc-shaped pipe of 1-cm in diameter (Segre 1961; Segre and Silberberg 1962a; Segre and Silberberg 1962b). This discovery has led various researchers to investigate this phenomenon.

In a later study by Karnis et al. (1966), it was shown that large particles can be focused near the center of a straight channel in higher flow rate, leaving smaller particles flowing near channel wall (see Fig. 8a). Particle migration is caused by the effect of shear gradient lift force (F_{LS}) that attracts particles toward the channel walls, and wall induced lift force (F_{LW}) that repulses them back toward the middle of the channel (see Fig. 8a). However, the effects of these two forces are dependent on particle mass, and particles of different sizes settle at different equilibrium positions within the channel.

In 2008, Di Carlo et al. (2007) and Bhagat et al. (2008) have separately shown that adding curvatures to the flow channel can lead to secondary vortices, i.e., Dean vortices that are perpendicular to the main flow stream (see Fig. 8b). Curved channels cause velocity mismatches between liquid elements that are near channel walls and those that are closer to the channel center (Di Carlo 2009; Zhang et al. 2016). Liquid elements near the channel center have higher inertia while the elements near the channel walls are relatively stagnant. This velocity mismatch results in two symmetrical secondary flows that are perpendicular to the liquid main flow. Therefore, particles in inertial microfluidics with spiral-shaped channel will follow these vortices in addition to the main flow. With this discovery and by following certain adjustments to the dimension and shape, relatively large particles can be
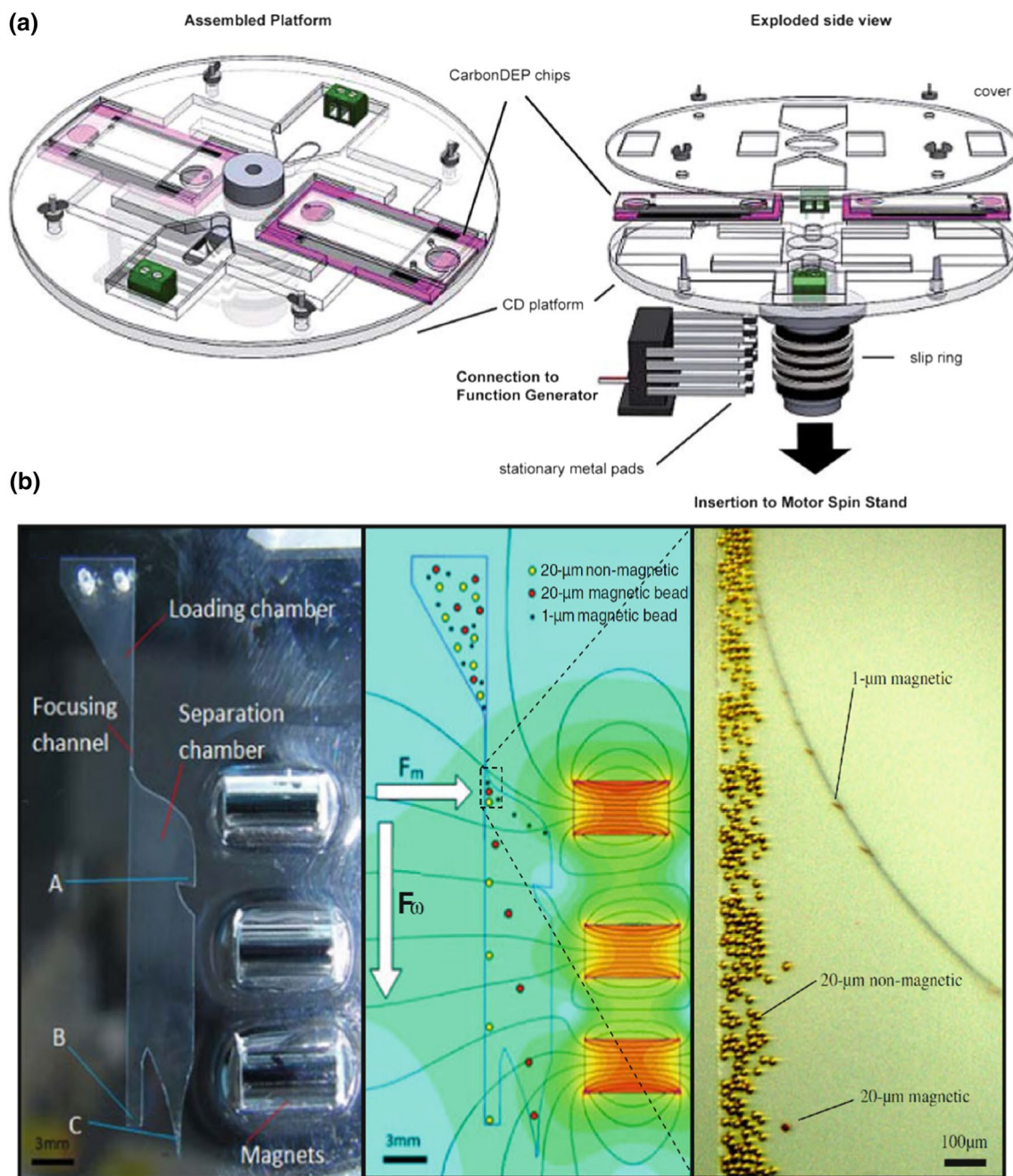
(a)

(b)

Fig. 7 Active cells/particles sorting on centrifugal microfluidic platform **a** dielectrophoresis (DEP) is integrated on the centrifugal microfluidic platform for selective particle/cell separation, slip rings and metal pads are utilized to provide the carbon electrodes with power **b** particle/cell sorting utilizing magnetic field, the design consist of loading chamber, focusing channel, separation chamber, and destination chamber *A*, *B*, and *C*, the figure also show the main forces effect particles movement, i.e., centrifugal force and magnetic force. **a** is adopted from Martinez-Duarte et al. (2010) with permission from Royal Society of Chemistry, **b** is adopted from Kirby et al. (2012) with permission from Springer

focused near the channel inner wall while leaving smaller particles to flow closer to the outer wall of the channel (see Fig. 8b) (Warkiani et al. 2014, 2016).

In most typical cases, microfluidic platforms are operated in the Stokes regime with negligible fluid inertia and Reynolds number (*Re*) (where $Re = \rho_f UH/\mu$; ρ_f is fluid density, *U* is average velocity, μ is dynamic viscosity, and *H* is the channel characteristic dimension). On the other hand, inertial microfluidics operate in approximate *Re* range from 1 up to 100, in other words between Stokes regime and turbulent regime (*Re* ~2000) (Zhang et al. 2016). For this kind of platforms, the influence of both
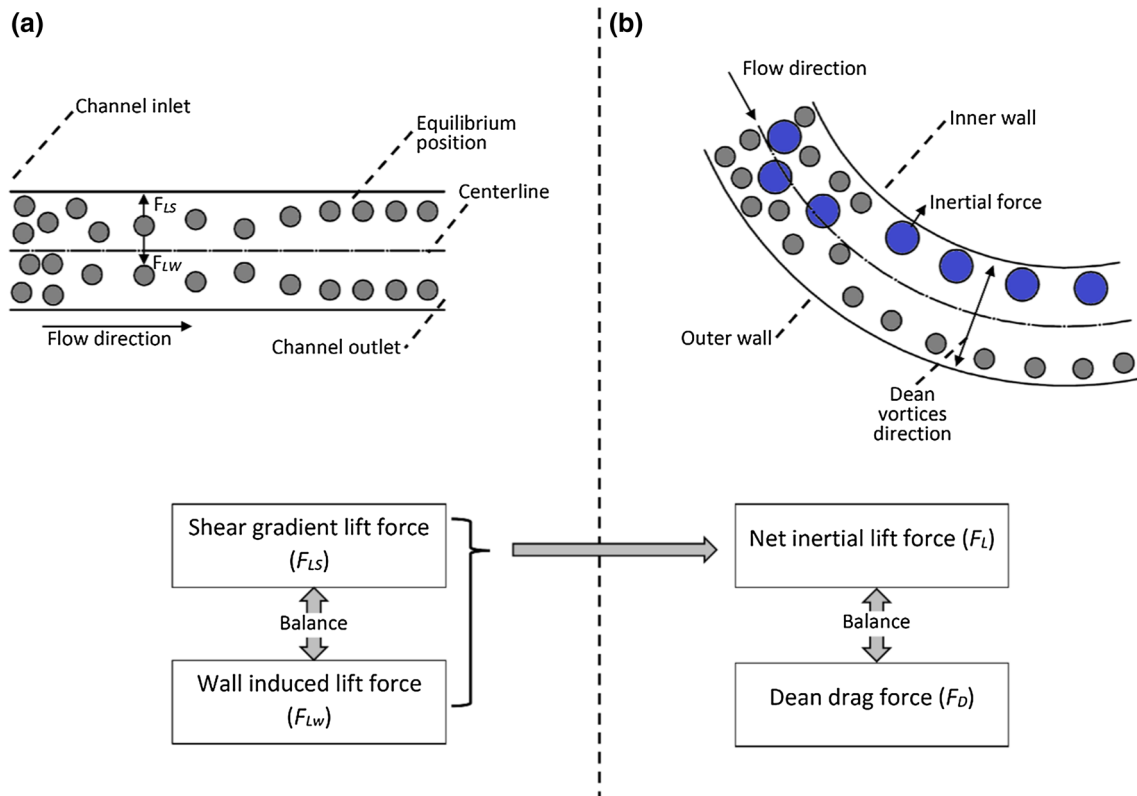
Fig. 8 Particle/cell migration in straight and curved channel (**a**) in straight channel, shear gradient lift force (F_{LS}) push particles toward the channel walls, and wall induced lift force (F_{LW}) that repulses them

back toward the center line of the channel (**b**) in spiral channel, the balance between net inertial lift force (F_L) and Dean drag force (F_D) causes particle migration to equilibrium position

inertia and viscosity of the fluid exist, causing particle migration during fluid flow in the microfluidic channel. The two effects on suspended particles: inertial migration and secondary flow are observed in this regime and are related to finite inertial forces (see Fig. 8).

When randomly dispersed particles with different sizes are injected and start flowing through a spiral, Dean vortices develop and the resulting drag forces cause the particles to follow the direction of these vortices in addition to the main stream flow.

Dean vortices strength are dependent on the Dean number (De), Reynolds number (Re), and channel aspect ratio (AR) (Zhang et al. 2016). Dean number is a dimensionless parameter which is a function of flow Reynolds number, channel hydraulic diameter (D_H), and the curvature of spiral channel (R_C), and it can by calculated by the following equation (Dean 1928):

$$De = Re\sqrt{\frac{D_H}{2R_C}} \tag{9}$$

Due to Dean vortices, particles are pushed back and forth between the side walls of the spiral. The velocity of this lateral flow is called Dean velocity (U_{Dean}) and it can

be calculated by the following equation (Warkiani et al. 2016):

$$U_{Dean} = 1.8 \times 10^{-4} De^{1.63} \tag{10}$$

When a particle travels in one direction between two opposite channel walls, it is said to have completed half a Dean cycle (L_{DC}) (Warkiani et al. 2016). A particle traveling from one wall to the opposite wall and then returning to the initial wall is considered to have completed a full L_{DC}. L_{DC} can be calculated as follows:

$$L_{DC} = 2w + h \tag{11}$$

where w is channel width and h is channel height. For particles to achieve an equilibrium position within a channel, the channel must have a minimum height calculated as follows:

$$l_C = \frac{U_F}{U_{Dean}}L_{DC} \tag{12}$$

where U_F is the average fluid velocity.

Finally, the Dean drag force can be calculated according to Stokes' law as:

$$F_D = 3\pi\mu U_{Dean}a_c \tag{13}$$

where a_c is particle diameter.

In curved channels, particles will be under the effect of both secondary flow due to Dean drag force, and inertial force (F_L). Inertial force is the balance of shear gradient lift force (F_{LS}) which push the particles toward channel walls, and wall induced lift force (F_{LW}) that repulses particles back toward channel center (Bhagat et al. 2008; Di Carlo et al. 2007). The net inertial force ($F_{L,nett}$) can be calculated as following (Bhagat et al. 2010):

$$F_{L,nett} = \frac{2\rho U_F^2 a_c^4}{D_H^2} \qquad (14)$$

In spiral channels, particles flowing within a curved sub-section will experience both lift force and drag force (which is caused by Dean vortices), leading to particle centrifugation (Zhang et al. 2016). Furthermore, since the channel curvature direction of the spiral is either outward toward the platform edge, or inward toward the platform center, the Dean vortices spinning direction is constant within each subsection. In a spiral, the Dean drag force changes as the particles move from one point in the spiral to another due to a change in the spiral curvature [see Eq. (9)]. However, as the spirals are relatively small, the change is negligible. As a result, the inertial force keeps particles in a specific cross-sectional equilibrium position and this position is under the effect of Dean drag force according to particle size. In other words, the ratio of inertial force to the Dean drag force, $R_f = a_c^3 R_c / D_H^3$ determines the relative position where particles of various sizes will gather within the channel. On a range of R_f from 0 to ∞, Dean drag force is dominant when R_f approaches 0, and this condition is true for particles with size much smaller than channel hydraulic diameter. In this case, Dean force drives small particles closer to the channel outer wall that is closer to the platform edge. On the other hand, as R_f approaches ∞, inertial force is dominant for large particles with diameter similar to channel hydraulic diameter. Therefore, large particles are flowing close to the inner wall of the curved channel which is closer to the platform center.

Spiral microfluidic platforms have been widely investigated by the Papautsky group (Bhagat et al. 2008, 2010; Kuntaegowdanahalli et al. 2009) and Lim and Han groups (Hou et al. 2013, 2015; Guan et al. 2013; Warkiani et al. 2014, 2015a, 2016) for particle/cell separation. A summary of the fabrication design, sample, applied flow rate, and reported results of the various platforms are summarized in Table 2. In two different works, Bhagat et al. (2008, 2010) from Papautsky group proposed sheath-less spiral channel for the separation of different size particles. The authors developed 5-loop and 10-loop spiral channels which have a rectangular cross section of width 100 μm by height 50 μm.

Table 2 Particle/cell separation methods on spiral platforms

First author	Turns	Width/height (μm)	Sample	Flow rate	Recovery/separation rate
Bhagat et al. (2008)	5	100/50	7.32 and 1.0 μm particles	0.02 mL/min, Re ~10	Complete separation is reported
Kuntaegowdanahalli et al. (2009)	5	500/130	10, 15, 20 μm particles; neu-roblastoma and glioma cells	~3 mL/min flow rate, Re 14.4	90% (particles) and 80% (cells), 90% (viability)
Bhagat et al. (2010)	10	100/50	6 μm particles	0.1 mL/min or Re ~ 20	Focusing only
Hou et al. (2013)	2	500/160	Blood (CTCs isolation)	0.05 mL/min	85% recovery, >98% viability
Warkiani et al. (2014)	2 with 3 stacked layers	500/160	Blood (CTCs isolation)	~1.5 mL/min	100%
Warkiani et al. (2014)	8	W 600, H inner/outer 80/130	Blood (CTCs isolation)	1.7 mL/min	80–90%
Hou et al. (2015)	2	500/80	Blood (bacteria isolation)	1.7 mL/min	>65%
Warkiani et al. (2015a)	8 with four spiral connected together	W 600, H inner/outer 80/130 for CHO cells, while W 450, H inner/outer 30/70 for yeast cells	CHO and Yeast cells	6 mL/min for a single spiral (~500 mL/min for 84 spiral chips)	>90%
Warkiani et al. (2016)	2 with 3 stacked layers	500/170	Blood (CTCs)	2.1 mL/min	≥85%
Schaap et al. (2016)	3	350/100	5, 10, 20 μm particles, and Algae cells	0.4–4 mL/min	96% (particles), 77% (Algae cells)

The 5-loop design was used to separate 7.32 and 1.9 μm particles, while the 10-loop design was implemented to focus 6 μm particles. Bhagat et al. (2010) reported high focusing throughput results of 2100 particles/s. Moreover, the system performance was validated for cell counting using SH-SY5Y neuroblastoma cells. In a related work from the same group, Kuntaegowdanahalli et al. (2009) developed a 5-loop spiral microchannel with a fork-shaped outlet for the separation of polystyrene particles of 10, 15, and 20 μm in sizes. As with any inertial platform, the proposed device utilizes the balance between inertial lift force and Dean drag force to focus particles near the side walls of the spiral channel. The authors reported respective recovery rates of 90 and 80% for polystyrene particles and neurogenic tumor cells. Moreover, the authors claimed that the platform achieved a throughput of around 1 million cells/min, which is higher than any cell sorting technique method currently commercially available at the time of publication.

Hou et al. (2013) from the Lim and Han group utilized spiral microfluidics, named as Dean flow fractionation (DFF), for continuous CTCs isolation from blood samples collected from patient with lung cancer. For the first time, sheath buffer was used in a spiral platform to facilitate the processing of blood samples with hematocrit levels of 20–25% compared to other works that reported as low hematocrit as 5%. The implementation of sheath buffer had resulting in a high throughput of 3 mL/h with the elimination of clogging issues, and CTCs recovery rate and viability of 85 and 98%, respectively. In a follow-up study, Hou et al. (2015) utilized a modified version of the platform for label-free bacteria isolation from host blood cells. Ribosomal RNA detection was then utilized to capture samples with low abundance pathogens (~100 per mL) from the processed blood sample without

the need for culturing or enzymatic amplification. The authors reported that in a test for bacteria identification from whole blood sample, an improved processing time of around 8 h was achieved compared to methods involving culturing or amplification. Also, the sensitivity of the platform was the same as that of methods involving culturing or amplification. A multiplexed setup of the same design was clinically validated and reported in a parallel research (Khoo et al. 2014), and the detailed procedure of the fabrication and implementation of multiplexed spiral microfluidics for CTCs isolation from blood sample was later reported in 2015 by Warkiani et al. (2016) (see Fig. 9a). The multiplexed platform achieved 85% recovery rate of CTCs cells at relatively high flow rate of 1.5 mL/min.

In an extensive theoretical and experimental study, Guan et al. (2013) has shown that spiral channels with rectangular cross sections has the limitation of low separation resolution, especially in close range of particle sizes (see Fig. 9a, b). Therefore, the authors proposed the use of channels with trapezoidal cross sections which generate stronger Dean drag force in the outer half of the channel, i.e., half opposite to the spiral channel center. This has led to higher separation distances between the different sized particles, i.e., better separation efficiency. In a continuation study, Warkiani et al. (2014) implemented trapezoidal spiral microfluidics for ultra-fast and label-free CTCs isolation (see Fig. 9b). The proposed platform was able to achieve an 80% recovery rate for cancer cells MCF-7, T24, and MDA-MB-231 from 7.5 mL of spiked blood in just eight minutes. Warkiani et al. (2015a) further demonstrated the implementation of multiplexing multi-trapezoid spiral with membrane-less microfiltration to eliminate the clogging limitation of using membrane filters. In their work, 48 spiral chips were integrated in one
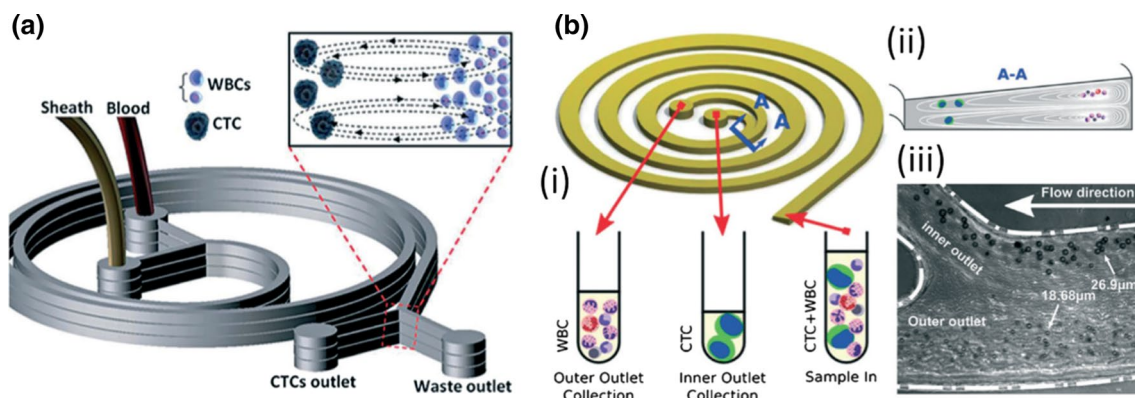

Fig. 9 Spiral microfluidic channel for passive particle/cell sorting **a** multi-layers spiral microfluidics with rectangular cross section, design used for CTCs isolation from blood sample **b** spiral microfluidic with trapezoidal cross sections, design used for CTCs isolation from WBC (*i*) full spiral design with one inlet and two outlets (*ii*) cross-sectional drawing (just before channel outlets) demonstrates focusing of different size particles (*iii*) experimental results of particles separation. **a** and **b** is adopted from Zhang et al. (2016) with permission from Royal Society of Chemistry

setup to increase the flow rate from 6 mL/min for single chip up to 500 mL/min. The integrated setup was successfully utilized for the separation of CHO (10–20 μm) and yeast (3–5 μm) cells with 90% separation efficiency. In a recent work by Schaap et al. (2016), a 3-loop spiral microfluidic with rectangular cross section of 350 μm width and 100 μm was proposed for particles and Algae cells sorting. The utilized polystyrene particles are spherical in shape with 5, 10, 20 μm diameter. The Algae cells sorted are from *Chlorella* (spherical shape), *Cyanothece* (Prolate spheroid), and *Monoraphidium* (Cylindrical). The authors reported 96 and 77% separation rate for polystyrene particle and Algae cell, respectively.

2.2.2 Multi-orifice microfluidic channel (microvortices)

Beside the utilization of curved microfluidic channel (spiral) to generate secondary flow, microvortices with inertial migration was also reported on microfluidic channel with single or multiple cavity/chamber on one or both sides. For summarized view, Table 3 lists the reported microvortices platforms according to their developing research group, platform structure, application, flow rate, and reported results. This idea was first invented and investigated for different application by the Chiu group (Shelby et al. 2003; Shelby and Chiu 2004; Chiu 2007). Shelby et al. (2003) proposed 30 μm height by 30 μm width straight

Table 3 Particle/cell separation methods on multi-orifice platforms

| Group leader	Structure	Application	Flow rate	Remarks
Shelby et al. (2003)	Single microchamber	Microvortex generation	1.08 mL/min	With low flow rate, the proposed design can achieve 12 m/s rotational velocity
Shelby and Chiu (2004), Chiu (2007)	Single microchamber	Particle/cell manipulation	0.001–2 mL/min	The proposed design was employed for cell separation and to study the centrifugation effect on cells
Lee et al. (2009a)	Multi-chamber on single side	Mixing	0.08 mL/min, $Re = 7.2$	Mixing range of 90% can be achieved in wide range of Reynold number (4.3–28.6)
Lee et al. (2009b)	Multi-chamber on single side	Focusing (red blood cells)	0.001–0.01 mL/min	The proposed platform requires sheath fluid to achieve 3D focusing
Lee et al. (2011c)	Multi-chamber on single side	Particles separation (4 and 10 μm)	0.016 mL/min	100% separation rate was achieved with a throughput of 111 particles/s. The proposed platform requires sheath liquid
Lee et al. (2011b)	Multi-chamber on single side	Blood plasma separation	0.02 mL/min	62% separation rate was achieved with a throughput of ~1.0×10^8 cells/min
Lee et al. (2013)	Multi-chamber on single side	Cancer cells separation	0.05–0.2 mL/min	99.1% recovery rate, 88.9% blood cells rejection rate, 1.1×10^8 cells/min throughput
Park et al. (2009)	Multi-chamber on two sides	Particle focusing (7 μm)	0.08 mL/min	Particles are focused near both sidewalls (at 0.6 from the centerline)
Park and Jung (2009)	Multi-chamber on two sides	Particle separation (7, 15 μm)	0.1 mL/min	~1–5×10^4 separation throughput, high recover rate of 90% but low purity 15%
Sim et al. (2011)	Multi-stage/multi- chamber on two sides	Particle separation (7, 15 μm)	0.061 and 0.102 mL/min	Compared to single stage, recover rate of 15 μm is improve to 88.7% with 89.1% purity
Moon et al. (2011)	Multi-chamber on two sides + DEP	Cancer cells separation	0.126 mL/min	75.18% recovery rate of MCF-7 cells. 162-fold of enrichment was reported
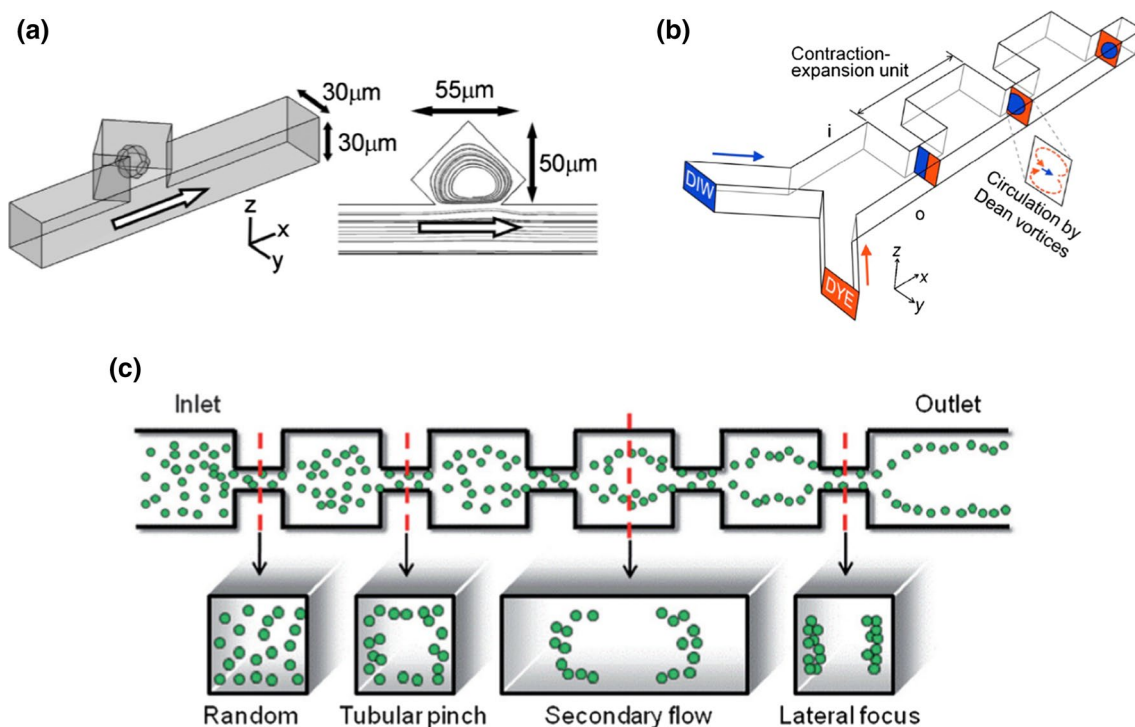
Fig. 10 Multi-orifice microfluidic channel (microvortices) **a** single microchamber (single vortex) by Chiu group, **b** multi-chamber on a single side of the channel by Park group, **c** multi-chamber on both side of the channel. **a** Is adopted from Shelby and Chiu (2004) with permission Royal Society of Chemistry, **b** is adopted from Lee et al. (2009a) with permission from AIP Publishing LLC, **c** is adopted from Park et al. (2009) with permission from Royal Society of Chemistry

microchannel with a single diamond-shaped chamber integrated on one side of the channel to generate high radial acceleration microvortices (Fig. 10a). The introduction of the microchamber creates detachment of fluid flow at the opening of the microchamber that will create recirculation/ vortex flow in the diamond chamber. With optimum microchamber dimensions and opening angle, flow velocity can be accelerated from 3 m/s in the main channel to 12 m/s in the microchamber. This microcirculation/microvortex was first reported to improve passive liquid mixing in a straight channel. To illustrate one of the potential applications of microvortex, Shelby employed red polystyrene beads and green slice beads with two different densities of 1.5 and 1.8–2.0 g/cm^3, respectively. When the flow rate of the main stream was increased from 1.5 to 20 m/s, the green beads was centrifuged toward the outer edge of the microchamber, while the red beads were concentrated at the center of the chamber. In later works, the group utilized the same idea to study the effect of centrifugation/vortices on different types of cells and molecules (Shelby and Chiu 2004; Chiu 2007). Compared to traditional centrifugation methods, microvotex method was able to reveal the different effect of centrifugation on a single-cell level, such as tensile stress that causes the relocation of intracellular

organelles, and shear stress that can cause physical changes to cell surface.

A series of microchambers, or as it also known as contraction–expansion array (CEA), integrated on a single side of the microchannel was first reported and investigated by the Park group (Fig. 10b). In their first work, Lee et al. (2009a) proposed CEA on a single side of the microchannel to perform laminar mixing between two liquids. Lee's theoretical and experimental analysis showed that the proposed CEA structure creates acceleration and deceleration of streamlines that result in Dean-like vortices at the entrance of contraction region. As what happen in a curved/ spiral channel, two vortices are generated, upper counterclockwise vortex and lower clockwise vortex. As shown in Fig. 10b, the two counter-rotating vortices shift the de-ionized water (DIW) toward the center of the channel where it will be surrounded by the fluorescein isothiocyanate (FITC/FYE). The author reported a mixing rate of 90% by utilizing 30 contraction–expansion array within a relatively wide range of Reynolds number of 4.3–28.6. In their following works, the group implemented the same microfluidic structure for three-dimensional hydrodynamic focusing of red blood cells (Lee et al. 2009b), inertial separation of different size polystyrene beads (Lee et al. 2011c), blood

plasma separation (Lee et al. 2011b), and label-free cancer cell separation from whole blood (Lee et al. 2013). For inertial focusing, the group utilized the balance between Dean force and inertial force to focus cells/particles based on their size.

Multi-orifice flow fractionation (MOFF) with axissymmetric CEA on both sides of the microchannel was first proposed by the Jung group in 2008 (Fig. 10c). Similar to the mechanism of single-sided CEA, double-sided CEA utilizes the balance between inertial force and microvortices on both sides to focus cells/particles in a specific path. This structure was first reported by Park et al. (2009) where they proposed a microchannel with 80 repeated contraction–expansion cycles for 7 μm polystyrene divinylbenzene (PS-DVB). According to the authors, this design offers continues separation of cells/particles with high throughput. Moreover, the focusing position was shown to move from the channel sides to the channel center when particle Reynolds number Re_p was increased from the range of 0.8–2.3 up to the range of 3.0–3.5. In their following work, Park implemented this MOFF platform to separate particles of different sizes, i.e., 2, 7 and 15 μm that replicates platelet, red blood cell, and white blood cell, respectively (Park and Jung 2009). For this application, the authors report that MOFF has the advantages of being a continues process, does not need sheath fluid, and having an intermediate flow rate of $1–5 \times 10^4$ particles/s compared to other separation methods (Park and Jung 2009). On the other hand, this platform showed low purity of 36.4% maximum for 15 μm particles. Furthermore, it was demonstrated that while enlarging the collection region increases the recovery rate, the level of separation purity dropped further to a low of 15.5%. To improve system performance, the authors suggested to have specific flow rate to separate each type of particles from the background mixture. Recently, Warkiani et al. (2015b) reported a CEA platform for Malaria parasite enrichment as a preprocessing step for qPCR assay. The CEA is utilized to focus and deplete the larger WBC cells, whereas unfocused smaller Malaria parasites are recovered from the center of the focusing channel. Warkiani et al. reported an impressive depletion rate of WBCs of 99.99%, with a throughput of 1 mL of lysed blood sample per 15 min.

Sim et al. (2011) and Moon et al. (2011) from the Park group proposed two different design improvements to the MOFF platform proposed by Park et al. 2009. Sim et al. (2011) developed a multi-stage-multi-orifice flow fractionation (MS-MOFF) platform where samples flow through two stages of CEA for better recovery rate. The design includes one CAE in the first stage, and two CAR in the second stage. With this MS-MOFF design, the final achieved recovery rate of 15 μm particle size was 88.5% with 89.1% purity, which were unachievable with a normal

MOFF platform. On the other hand, Moon et al. (2011) integrated MOFF with dielectrophoretic (DEP) to improve the recovery rate of MOFF. This integrated platform was implemented to separate breast cancer cells (MCF-7) from spiked blood sample. The authors reported 162-fold of MCF-7 enrichment at a flow rate of 126 μL/min.

For further improvement in term of throughput of CEA platform, Mach et al. (2011) proposed an array of CEA where multiple CEA channels are connected in parallel with a single input and a single output. However, Mach et al. implemented the microvortices to trap larger particle and not to focus it. In other words, as soon as larger particles/cells reach a microvortex, it is centrifuged near the vortex center and stays there, while small particles flow with the main stream. This idea was successfully implemented to trap targeted particles, then fluorescent labeling it by a medium exchange process without the need for manual pipetting and washing steps. Moreover, this method achieved high throughput in the range of mL/min. To release trapped particles/cells, the flow rate is decreased to weaken microvortices and let particles/cells escape to the main flow. This method was utilized to isolate CTCs and mesothelial cells from background mixture (Mach et al. 2011; Sollier et al. 2014; Che et al. 2013).

3 Summary and future outlook

This paper has reviewed the microfluidic platforms and centrifugation approaches for particle/cell separation. Centrifugation approaches are methods that utilize the physical centrifugation process on microfluidic platforms such as in microfluidic CD, or approaches that utilize liquid centrifugation effect which results from the Dean effect for cell/particle separation such as in spiral and multi-orifice microfluidics.

The various implementation of particle/cell separation on centrifugal microfluidic platforms are either passive or active in nature. Table 1 in Sect. 2.1 shows the various methods reviewed. Passive methods include density-based sedimentation, separation by physical size, and separation through immunoaffinity, whereas active methods include DEP or magnetic based separation. Most reported techniques showed that the centrifugal microfluidic platform is most suitable when a preparation step of a raw sample is required to be integrated on the same platform. For example, the fractionation of blood sample to its sub-component can be easily performed with simple one-chamber designs. Nevertheless, centrifugal microfluidic platforms have also demonstrated the ability to perform single-particle/cell separation and particle/cell observations using simple passive structure such as V-shaped cups, inertial focusing, or by the implementation of a DGM.

Table 4 Microfluidic platforms for CTCs isolation

References	Platform type	Separation method	Sample type/preparation	Processed volume	Processing time	Test repetition (n)	CTCs recovery rate (%)
Lee et al. (2014)	Centrifugal microfluidic platform	Membrane filter	MCF-7 breast cancer cells spiked in PBS and whole blood sample (Laboratory experiment). Whole blood sample from patient with lung cancer and gastric cancer (Clinical experiment)	3 mL	20 s filtration time. 50.5 min for washing, blocking, staining and cells analysis	3	44–84 (according to flow rate and sample type)
Aguirre et al. (2015)	Centrifugal microfluidic platform	Immunoaffinity, and inertial cell sorting	250–1050 MCF-7 breast cancer cells spiked in diluted blood. Dilution rate is 2 and 5% v/v in PBS buffer. 200:1 beads to cancer cells ration was implemented	1 mL	Not reported	3	98.7
Park et al. (2014)	Centrifugal microfluidic platform	Immunoaffinity, and density gradient medium (DGM)	Whole blood sample spiked with MCF-7 breast cancer and HCC827 lung cancer cell. The blood was mixed with microbeads. Microbeads are covered with anti-EPCAM to capture CTCs	5 mL	78 min	3	90–95 for MCF-7 and HCC827, respectively
Kirby et al. (2015)	Centrifugal microfluidic platform	Centrifugo-magnetophoresis, continuous sedimentation	Whole blood sample spiked with MCF-7 breast cancer. The sample is mixed with activated 4.5 µm magnetic beads	3 µL each set	10 min (focusing time only without CTCs-beads incubation time)	5	80–88 according to sample concentration
Hou et al. (2013)	Inertial microfluidics (spiral)	Spiral channel, sheath flow	Whole blood spiked with CTCs, and whole blood from patient with lung cancer. Blood was diluted to 20% hematocrit (only 2 dilution of whole blood)	3 mL	1 h	20	85
Khoo et al. (2014)	Inertial microfluidics (spiral)	Spiral channel, sheath flow	Blood from advance metastatic breast and lung cancers at 2× concentration were fractionated, lysed, and resuspended in 3.75 mL PBS	7.5 mL	5 min	56	100
Warkiani et al. (2016)	Inertial microfluidics (spiral)	Spiral channel, sheath flow	System evaluated with: microbeads 6, 10, 15 µm and lysed blood sample spiked with different CTCs lines	7.5 mL	12.5 min	15 breast cancer and 15 lung cancer	85
Warkiani et al. (2014)	Inertial microfluidics (trapezoidal spiral)	Trapezoidal spiral	Whole blood sample was lysed and spiked with MCF-7, T24 and MDA-MB-231 CTC line cells (breast and lung cancer cells)	7.5 mL	8 min	10	80
Lee et al. (2013)	Multi-orifice microfluidic	Multi-orifice microfluidic with focusing flow (sheath flow)	Whole blood sample with 45% hematocrit was spiked with MCF-7, SK-BR-3, and HCC70 breast cancer cells	No specific volume (system can process 6 mL in 1 h)	1 h for 6 mL of sample	3	99.1

Table 4 continued

References	Platform type	Separation method	Sample type/preparation	Processed volume	Processing time	Test repetition (n)	CTCs recovery rate (%)
Moon et al. (2011)	Multi-orifice microfluidic	Multi-orifice microfluidic with DEP	Whole blood sample was processed to have the following cells concentration: 10, 1, 1 ($\times 10^3$ μL^{-1}) for RBC, WBC, and MCF-7, respectively	No specific volume (system can process 0.7 mL in 1 h)	1 h for 0.7 mL of sample		75.18
Mach et al. (2011)	Multi-orifice microfluidic	Multi-orifice microfluidic, multi-line in parallel	10 mL of whole blood sample was diluted to 5% v/v (i.e., 0.5 mL of whole blood), and spike with MCF-7 cancer cell	10 mL can be processed	Less than 30 min	6	~10–20
Sollier et al. (2014)	Multi-orifice microfluidic	Multi-orifice microfluidic, multi-line in parallel	Whole blood sample from healthy donors was diluted in a range of 5^x–40^x and spiked with breast or lung cancer. Blood from patients with breast and lung cancer was used for system evaluation	7.5	20 min	4 breast cancer and 8 lung cancer	~20

The main advantages of using the centrifugal microfluidic platforms for particle/cell separation include simple design and fabrication process, allowance for the integration of multi-processing stages of mixing, valving, centrifugation…,etc., improved portability of the proposed methods, requires less human interaction, and includes a wide range of implementable unit/operations that can be utilized in different applications. On the other hand, the main disadvantage of using centrifugal microfluidic platforms for particle/cell separation is the limited space available on the platform for sample, reagents, and other fluids/components. Even though some authors reported the ability to process sample volume of around 5 mL, processing such sample volumes limits the number of processes that can be multiplexed on the same platform.

Inertial microfluidic platforms are categorized into spiral microfluidics and multi-orifice microfluidics, or microvotices. Table 2 in Sect. 2.2.1 shows the various implementation of spiral microfluidics, while Table 3 in Sect. 2.2.2 shows the works performed using multi-orifice. In general, inertial microfluidics is more suitable than centrifugal microfluidics when it comes to processing samples of high volumes, e.g., for CTCs isolation. This is due to the fact that samples are loaded using syringe pumps which can cater to a wider range of sample volumes required for any kind of application.

Many works have demonstrated that inertial microfluidics is suitable for particles/cell separation. Some examples are the separation of CTCs, WBC, Algae, and bacteria with high recovery and viability rate. Some studies have also highlighted that spiral microfluidic designs can be easily adapted for different applications by adjusting the spiral cross-sectional, dimension, length, and flow rate. Meanwhile, multi-orifice has been reported to be also designed with different structures to suit specific application. Variations of the designs include single chamber (single vortex), multi-chamber on a single side of the channel, and multi-chamber on both sides of the channel.

The many advantages of inertial, or spiral and multi-orifice microfluidics include simple design and fabrication, the ability to process large sample volumes, high throughput, high recovery rate, and the ability for multiplexing for improved performance. However, the use of syringe pump has reduced the flexibility of the platform in integrating preprocessing steps for more involved processes.

As both types of microfluidic platforms, namely centrifugal microfluidic platform and inertial microfluidic platform, have their advantages and disadvantages, the requirement of the application should be carefully considered prior to platform selection. For example, to design a point-of-care application for low resource

environment, and preprocessing is required, then centrifugal microfluidic platforms should be a better choice. On the other hand, if the desired platform is the miniaturization of commercially available machines with reduced processing time, with relatively high volume of sample, then inertial microfluidic platform is the better choice. Due to the importance of CTCs isolation and retrieval for early cancer diagnosis, the proposed microfluidic methods for CTCs isolation are summarized in Table 4.

In summary, microfluidic platforms are capable of (1) having high portability, (2) wide range of applicable operations, (3) integrating preprocessing stages, (4) processing relatively high sample volume, (5) high throughput, and (6) high recovery and viability rate. With proper consideration to the requirement of the application, various particle/cell separation platforms can be accomplished.

References

Aguirre GR, Efremov V, Kitsara M, Ducrée J (2015) Integrated micromixer for incubation and separation of cancer cells on a centrifugal platform using inertial and dean forces. Microfluid Nanofluid 18(3):513–526

Amasia M, Madou M (2010) Large-volume centrifugal microfluidic device for blood plasma separation. Bioanalysis 2(10):1701–1710

Arosio P, Müller T, Mahadevan L, Knowles TP (2014) Density-gradient-free microfluidic centrifugation for analytical and preparative separation of nanoparticles. Nano Lett 14(5):2365–2371

Ashworth T (1869) A case of cancer in which cells similar to those in the tumours were seen in the blood after death. Aust Med J 14(3):146–149

Bhagat AAS, Kuntaegowdanahalli SS, Papautsky I (2008) Continuous particle separation in spiral microchannels using dean flows and differential migration. Lab Chip 8(11):1906–1914

Bhagat AAS, Kuntaegowdanahalli SS, Kaval N, Seliskar CJ, Papautsky I (2010) Inertial microfluidics for sheath-less high-throughput flow cytometry. Biomed Microdevice 12(2):187–195

Boycott A (1920) Sedimentation of blood corpuscles. Nature 104:532

Brenner T, Glatzel T, Zengerle R, Ducree J (2005) Frequency-dependent transversal flow control in centrifugal microfluidics. Lab Chip 5(2):146–150. doi:10.1039/b406699e

Burger R, Ducrée J (2012) Handling and analysis of cells and bioparticles on centrifugal microfluidic platforms. Expert Rev Mol Diagn 12(4):407–421. doi:10.1586/erm.12.28

Burger R, Kijanka G, Sheils O, O'Leary J, Ducrée J (2011) Arrayed capture, assaying and binary counting of cells in a stopped-flow sedimentation mode. In: 15th International conference on miniaturized systems for chemistry and life sciences (uTAS). Seattle, pp 2–6

Burger R, Kirby D, Glynn M, Nwankire C, O'Sullivan M, Siegrist J, Kinahan D, Aguirre G, Kijanka G, Gorkin RA (2012a) Centrifugal microfluidics for cell analysis. Curr Opin Chem Biol 16(3):409–414

Burger R, Reith P, Kijanka G, Akujobi V, Abgrall P, Ducrée J (2012b) Array-based capture, distribution, counting and multiplexed assaying of beads on a centrifugal microfluidic platform. Lab Chip 12(7):1289–1295

Che J, Mach AJ, Go DE, Talati I, Ying Y, Rao J, Kulkarni RP, Di Carlo D (2013) Microfluidic purification and concentration of malignant pleural effusions for improved molecular and cytomorphological diagnostics. PLoS ONE 8(10):e78194

Chiu DT (2007) Cellular manipulations in microvortices. Anal Bioanal Chem 387(1):17–20

Dean W (1928) Fluid motion in a curved channel. In: Proceedings of the Royal Society of London A: mathematical, physical and engineering sciences, vol 787. The Royal Society, pp 402–420

Di Carlo D (2009) Inertial microfluidics. Lab Chip 9(21):3038–3046

Di Carlo D, Irimia D, Tompkins RG, Toner M (2007) Continuous inertial focusing, ordering, and separation of particles in microchannels. Proc Natl Acad Sci 104(48):18892–18897

Ducrée J, Haeberle S, Lutz S, Pausch S, Von Stetten F, Zengerle R (2007) The centrifugal microfluidic Bio-Disk platform. J Micromech Microeng 17(7):S103–S115

Furutani S, Nagai H, Takamura Y, Kubo I (2010) Compact disk (CD)-shaped device for single cell isolation and PCR of a specific gene in the isolated cell. Anal Bioanal Chem 398(7–8):2997–3004

Glynn M, Nwankire C, Lemass K, Kinahan DJ, Ducrée J (2015) Cluster size distribution of cancer cells in blood using stopped-flow centrifugation along scale-matched gaps of a radially inclined rail. Microsyst Nanoeng 1. doi:10.1038/micronano.2015.18

Guan G, Wu L, Bhagat AA, Li Z, Chen PC, Chao S, Ong CJ, Han J (2013) Spiral microchannel with rectangular and trapezoidal cross-sections for size based particle separation. Scientific reports 3

Haeberle S, Brenner T, Zengerle R, Ducrée J (2006) Centrifugal extraction of plasma from whole blood on a rotating disk. Lab Chip 6(6):776–781

Hou HW, Warkiani ME, Khoo BL, Li ZR, Soo RA, Tan DS-W, Lim WT, Han J, Bhagat AAS, Lim CT (2013) Isolation and retrieval of circulating tumor cells using centrifugal forces. Scientific reports 3

Hou HW, Bhattacharyya RP, Hung DT, Han J (2015) Direct detection and drug-resistance profiling of bacteremias using inertial microfluidics. Lab Chip 15(10):2297–2307

Hyun K-A, Jung H-I (2014) Advances and critical concerns with the microfluidic enrichments of circulating tumor cells. Lab Chip 14(1):45–56

Jiang M, Mazzeo AD, Drazer G (2015) Centrifugal deterministic lateral displacement separation system. arXiv preprint arXiv:150706027

Karnis A, Goldsmith H, Mason S (1966) The flow of suspensions through tubes: v. Inertial effects. Can J Chem Eng 44(4):181–193

Khoo BL, Warkiani ME, Tan DS, Bhagat AA, Irwin D, Lau DP, Lim AS, Lim KH, Krisna SS, Lim WT, Yap YS, Lee SC, Soo RA, Han J, Lim CT (2014) Clinical validation of an ultra high-throughput spiral microfluidics for the detection and enrichment of viable circulating tumor cells. PLoS One 9(7):e99409. doi:10.1371/journal.pone.0099409

Kim J, Kido H, Rangel RH, Madou MJ (2008) Passive flow switching valves on a centrifugal microfluidic platform. Sens Actuators B Chem 128(2):613–621. doi:10.1016/j.snb.2007.07.079

Kim T-H, Hwang H, Gorkin R, Madou M, Cho Y-K (2013) Geometry effects on blood separation rate on a rotating disc. Sens Actuators B Chem 178:648–655

Kinahan D, Kilcawley N, Glynn M, Kirby D, Ducree J (2014a) Isolation of white blood cells using paper-triggered dissolvable-film valves on a centrifugal platform. In: 18th International conference on miniaturized systems for chemistry and life sciences (uTAS). Texas, pp 1425–1427

Kinahan DJ, Kearney SM, Glynn MT, Ducrée J (2014b) Spira mirabilis enhanced whole blood processing in a lab-on-a-disk. Sens Actuators, A 215:71–76

Kirby D, Siegrist J, Kijanka G, Zavattoni L, Sheils O, O'Leary J, Burger R, Ducrée J (2012) Centrifugo-magnetophoretic particle separation. Microfluid Nanofluid 13(6):899–908

Kirby D, Glynn M, Kijanka G, Ducrée J (2015) Rapid and cost-efficient enumeration of rare cancer cells from whole blood by low-loss centrifugo-magnetophoretic purification under stopped-flow conditions. Cytom Part A 87(1):74–80

Kubo I, Furutani S, Nagai H (2009) The activity determination of single cell by isolation and cultivation on a centrifugal flow disk. ECS Trans 16(17):1–8

Kuntaegowdanahalli SS, Bhagat AAS, Kumar G, Papautsky I (2009) Inertial microfluidics for continuous particle separation in spiral microchannels. Lab Chip 9(20):2973–2980

Kuo J-N, Chen X-F (2015) Plasma separation and preparation on centrifugal microfluidic disk for blood assays. Microsyst Technol 21(11):2485–2494

Kuo J-N, Li B-S (2014) Lab-on-CD microfluidic platform for rapid separation and mixing of plasma from whole blood. Biomed Microdevice 16(4):549–558

Lee MG, Choi S, Park J-K (2009a) Rapid laminating mixer using a contraction-expansion array microchannel. Appl Phys Lett 95(5):051902

Lee MG, Choi S, Park J-K (2009b) Three-dimensional hydrodynamic focusing with a single sheath flow in a single-layer microfluidic device. Lab Chip 9(21):3155–3160

Lee BS, Lee YU, Kim H-S, Kim T-H, Park J, Lee J-G, Kim J, Kim H, Lee WG, Cho Y-K (2011a) Fully integrated lab-on-a-disc for simultaneous analysis of biochemistry and immunoassay from whole blood. Lab Chip 11(1):70–78

Lee MG, Choi S, Kim H-J, Lim HK, Kim J-H, Huh N, Park J-K (2011b) Inertial blood plasma separation in a contraction–expansion array microchannel. Appl Phys Lett 98(25):253702

Lee MG, Choi S, Park J-K (2011c) Inertial separation in a contraction–expansion array microchannel. J Chromatogr A 1218(27):4138–4143

Lee MG, Shin JH, Bae CY, Choi S, Park J-K (2013) Label-free cancer cell separation from human whole blood using inertial microfluidics at low shear stress. Anal Chem 85(13):6213–6218

Lee A, Park J, Lim M, Sunkara V, Kim SY, Kim GH, Kim M-H, Cho Y-K (2014) All-in-one centrifugal microfluidic device for size-selective circulating tumor cell isolation with high purity. Anal Chem 86(22):11349–11356

Li T, Zhang L, Leung KM, Yang J (2010) Out-of-plane microvalves for whole blood separation on lab-on-a-CD. J Micromech Microeng 20(10):105024

Mach AJ, Kim JH, Arshi A, Hur SC, Di Carlo D (2011) Automated cellular sample preparation using a centrifuge-on-a-chip. Lab Chip 11(17):2827–2834

Madou M, Zoval J, Jia G, Kido H, Kim J, Kim N (2006) Lab on a CD. Annu Rev Biomed Eng 8:601–628

Martinez-Duarte R, Gorkin RA III, Abi-Samra K, Madou MJ (2010) The integration of 3D carbon-electrode dielectrophoresis on a CD-like centrifugal microfluidic platform. Lab Chip 10(8):1030–1043

Moen ST, Hatcher CL, Singh AK (2016) A centrifugal microfluidic platform that separates whole blood samples into multiple removable fractions due to several discrete but continuous density gradient sections. PLoS ONE 11(4):e0153137

Moon H-S, Kwon K, Kim S-I, Han H, Sohn J, Lee S, Jung H-I (2011) Continuous separation of breast cancer cells from blood samples using multi-orifice flow fractionation (MOFF) and dielectrophoresis (DEP). Lab Chip 11(6):1118–1125

Morijiri T, Yamada M, Hikida T, Seki M (2013) Microfluidic counter-flow centrifugal elutriation system for sedimentation-based cell separation. Microfluid Nanofluid 14(6):1049–1057

Nwankire CE, Maguire I, Kernan D, Glynn M, Kirby D, Ducree J (2015a) SIZE-and deformability-based particle sorting by strategic design of obstacle arrays in continuous centrifugal sedimentation mode. In: Transducers-2015 18th international conference on solid-state sensors, actuators and microsystems (TRANSDUCERS). IEEE, pp 1854–1856

Nwankire CE, Venkatanarayanan A, Glennon T, Keyes TE, Forster RJ, Ducrée J (2015b) Label-free impedance detection of cancer cells from whole blood on an integrated centrifugal microfluidic platform. Biosens Bioelectron 68:382–389

Park J-S, Jung H-I (2009) Multiorifice flow fractionation: continuous size-based separation of microspheres using a series of contraction/expansion microchannels. Anal Chem 81(20):8280–8288

Park J-M, Kim B-C, Lee J-G, Ko C (2008) One-step white blood cell separation from whole blood on centrifugal microfluidic. Paper presented at the NSTI-nanotech Boston, 1–5 June 2008

Park J-S, Song S-H, Jung H-I (2009) Continuous focusing of microparticles using inertial lift force and vorticity via multi-orifice microfluidic channels. Lab Chip 9(7):939–948

Park J-M, Kim MS, Moon H-S, Yoo CE, Park D, Kim YJ, Han K-Y, Lee J-Y, Oh JH, Kim SS (2014) Fully automated circulating tumor cell isolation platform with large-volume capacity based on lab-on-a-disc. Anal Chem 86(8):3735–3742

Riegger L, Grumann M, Steigert J, Lutz S, Steinert C, Mueller C, Viertel J, Prucker O, Rühe J, Zengerle R (2007) Single-step centrifugal hematocrit determination on a 10-$ processing device. Biomed Microdevice 9(6):795–799

Sajeesh P, Sen AK (2014) Particle separation and sorting in microfluidic devices: a review. Microfluid Nanofluid 17(1):1–52

Schaap A, Dumon J, Den Toonder J (2016) Sorting algal cells by morphology in spiral microchannels using inertial microfluidics. Microfluid Nanofluid 20(9):125

Segre G (1961) Radial particle displacements in Poiseuille flow of suspensions. Nature 189:209–210

Segre G, Silberberg A (1962a) Behaviour of macroscopic rigid spheres in Poiseuille flow part 1. Determination of local concentration by statistical analysis of particle passages through crossed light beams. J Fluid Mech 14(01):115–135

Segre G, Silberberg A (1962b) Behaviour of macroscopic rigid spheres in Poiseuille flow part 2. Experimental results and interpretation. J Fluid Mech 14(01):136–157

Shamloo A, Selahi A, Madadelahi M (2016) Designing and modeling a centrifugal microfluidic device to separate target blood cells. J Micromech Microeng 26(3):035017

Shelby JP, Chiu DT (2004) Controlled rotation of biological micro- and nano-particles in microvortices. Lab Chip 4(3):168–170

Shelby JP, Lim DS, Kuo JS, Chiu DT (2003) Microfluidic systems: high radial acceleration in microvortices. Nature 425(6953):38

Siegrist J, Burger R, Kirby D, Zavattoni L, Kijanka G, Ducrée J (2011) Stress-free centrifugomagnetic 2D-separation of cancer cells in a stopped-flow mode. In: 15th International conference on miniaturized systems for chemistry and life sciences (uTAS). Seattle, pp 2–6

Sim TS, Kwon K, Park JC, Lee J-G, Jung H-I (2011) Multistage-multiorifice flow fractionation (MS-MOFF): continuous size-based separation of microspheres using multiple series of contraction/expansion microchannels. Lab Chip 11(1):93–99

Smith S, Mager D, Perebikovsky A, Shamloo E, Kinahan D, Mishra R, Torres Delgado SM, Kido H, Saha S, Ducrée J (2016) CD-based microfluidics for primary care in extreme point-of-care settings. Micromachines 7(2):22

Sollier E, Go DE, Che J, Gossett DR, O'Byrne S, Weaver WM, Kummer N, Rettig M, Goldman J, Nickols N (2014) Size-selective collection of circulating tumor cells using Vortex technology. Lab Chip 14(1):63–77

Steigert J, Grumann M, Dube M, Streule W, Riegger L, Brenner T, Koltay P, Mittmann K, Zengerle R, Ducrée J (2006) Direct hemoglobin measurement on a centrifugal microfluidic platform for point-of-care diagnostics. Sens Actuators, A 130:228–233

Steigert J, Brenner T, Grumann M, Riegger L, Lutz S, Zengerle R, Ducrée J (2007) Integrated siphon-based metering and sedimentation of whole blood on a hydrophilic lab-on-a-disk. Biomed Microdevice 9(5):675–679

Strohmeier O, Keller M, Schwemmer F, Zehnle S, Mark D, von Stetten F, Zengerle R, Paust N (2015a) Centrifugal microfluidic platforms: advanced unit operations and applications. Chem Soc Rev 44:6187–6229

Strohmeier O, Keller M, Schwemmer F, Zehnle S, Mark D, von Stetten F, Zengerle R, Paust N (2015b) Centrifugal microfluidic platforms: advanced unit operations and applications. Chem Soc Rev 44(17):6187–6229

Tang M, Wang G, Kong S-K, Ho H-P (2016) A review of biomedical centrifugal microfluidic platforms. Micromachines 7(2):26

Thio THG, Soroori S, Ibrahim F, Al-Faqheri W, Soin N, Kulinsky L, Madou M (2013) Theoretical development and critical analysis of burst frequency equations for passive valves on centrifugal microfluidic platforms. Med Biol Eng Comput 51(5):525–535

Tomlinson MJ, Tomlinson S, Yang XB, Kirkham J (2013) Cell separation: terminology and practical considerations. J Tissue Eng 4:2041731412472690

Warkiani ME, Guan G, Luan KB, Lee WC, Bhagat AAS, Chaudhuri PK, Tan DS-W, Lim WT, Lee SC, Chen PC (2014) Slanted spiral microfluidics for the ultra-fast, label-free isolation of circulating tumor cells. Lab Chip 14(1):128–137

Warkiani ME, Tay AKP, Guan G, Han J (2015a) Membrane-less microfiltration using inertial microfluidics. Scientific reports 5

Warkiani ME, Tay AKP, Khoo BL, Xiaofeng X, Han J, Lim CT (2015b) Malaria detection using inertial microfluidics. Lab Chip 15(4):1101–1109

Warkiani ME, Wu L, Tay AKP, Han J (2015c) Large volume microfluidic cell sorting. Annu Rev Biomed Eng 17(1):1–34

Warkiani ME, Khoo BL, Wu L, Tay AKP, Bhagat AAS, Han J, Lim CT (2016) Ultra-fast, label-free isolation of circulating tumor cells from blood using spiral microfluidics. Nat Protoc 11(1):134–148

Zhang J, Guo Q, Liu M, Yang J (2008) A lab-on-CD prototype for high-speed blood separation. J Micromech Microeng 18(12):125025

Zhang J, Yan S, Yuan D, Alici G, Nguyen N-T, Warkiani ME, Li W (2016) Fundamentals and applications of inertial microfluidics: a review. Lab Chip 16(1):10–34

Zhao Y, Schwemmer F, Zehnle S, von Stetten F, Zengerle R, Paust N (2015) Centrifugo-pneumatic sedimentation, re-suspension and transport of microparticles. Lab Chip 15(21):4133–4137